TÜBİTAK

Turkish Journal of Earth Sciences

http://journals.tubitak.gov.tr/earth/

Research Article

Turkish J Earth Sci
(2017) 26: 147-169

doi:10.3906/yer-1602-2

Relationships between sequence stratigraphy and diagenesis of corals and foraminifers in the Middle Eocene, northern Egypt

Mohamed TAWFIK[1,*], Abdelbaset S. EL-SOROGY[1,2], Mahmoud MOUSSA[3]

[1]Department of Geology, Faculty of Science, Zagazig University, Zagazig, Egypt

[2]Department of Geology and Geophysics, College of Science, King Saud University, Riyadh, Saudi Arabia

[3]Energy and Mineral Resources Group, Geological Institute, RWTH-Aachen University, Aachen, Germany

Received: 06.02.2016 • **Accepted/Published Online:** 11.04.2017 • **Final Version:** 15.06.2017

Abstract: Outcrops of the Middle Eocene in northern Egypt represent a Tethyan reef-rimmed carbonate platform with bedded inner-platform facies. The diagenesis of these outcrops was studied in detail. The facies are characterized by a reef core, back reef and outer lagoon, shoal, inner lagoon, and tidal flat carbonate sequences. The diagenetic sequences on the scleractinian corals and foraminifers were thoroughly examined. These sequences show various diagenetic features during episodes of fluctuating sea levels and appear to be related to the primary composition of the studied components and the transgressive-regressive cycles. The carbonate diagenetic history of the examined samples successively includes marine-phreatic, mixed marine-meteoric, and shallow burial diagenesis. Most of the coral samples are affected by micritization and neomorphism and most of the foraminiferal samples are affected by micritization, dolomitization, glauconitization, or cementation. A sequence-stratigraphic analysis was carried out by integrating field and laboratory studies. The investigated sections were subdivided into three third-order sequences named S1, S2, and S3. The distribution of diagenetic fabrics was compared to a sequence stratigraphic framework. This has resulted in, for example, recording isopachous cement and autochthonous glauconitization mostly in the transgressive parts, while dolomitization, drusy cement, and biomoldic and vuggy porosities are recorded in the regressive parts; dedolomitization, allochthonous glauconitization, and ferrugination processes occurred at the sequence boundaries.

Keywords: Middle Eocene, Egypt, lithofacies association, diagenetic sequence, corals, foraminifers, depositional sequences, sequence boundaries

1. Introduction

The Middle Eocene successions in northern Egypt are dominated by shallow marine carbonates and are represented by different marine facies (limestone, shale, and chalk with marl interbeds). They are also characterized by corals, bryozoan, benthic large foraminifers, and other fossils. The studied sections are located in the region between Wadi el Ramliya in the Eastern Desert to Cairo to Wadi el Hitan in the Western Desert in the Fayum province (Figure 1). These sections exhibit vertical variations in lithology and fossils (Figure 2) that lead to its subdivision into sequences. The diagenetic processes are represented in all studied sections, which contain both early and late stage diagenesis. These make it possible for them to reform their compositional features and main texture. The diagenetic features seem to have arisen in four diagenetic environments. There are marine phreatic, meteoric, mixed marine-meteoric, and shallow burial. As noted by Morad et al. (2012), the connection between diagenesis and sequence stratigraphy is theoretically possible because factors that prevailed over the stratigraphic sections exert deep effects on the diagenetic variations in these sections.

Almost all carbonates undergo significant diagenesis even at a moderate burial, and in many cases these are recrystallized (Bathurst, 1975). Therefore, nearly all the studies of ancient limestone include the clarification of both the diagenetic history and the original depositional texture (Evans and Ginsburg, 1987; Steinhauff et al., 1999, Basilone, 2009). The relation of diagenesis to sequence stratigraphy has been studied recently for both carbonates and siliciclastics (e.g., Morad, 1998; Tucker and Booler, 2002; Khalifa et al., 2014). According to Vail et al. (1977) and Ketzer et al. (2003), short-term variations in diagenetic parameters take place within the time spent during sequence deposition (i.e. third- or fourth-order relative sea-level cycles). The regional stratigraphy and the diagenetic processes of the studied sections have been examined by many researchers, (e.g., Haggag, 1990, 1992;

* Correspondence: tawfik3030@gmail.com

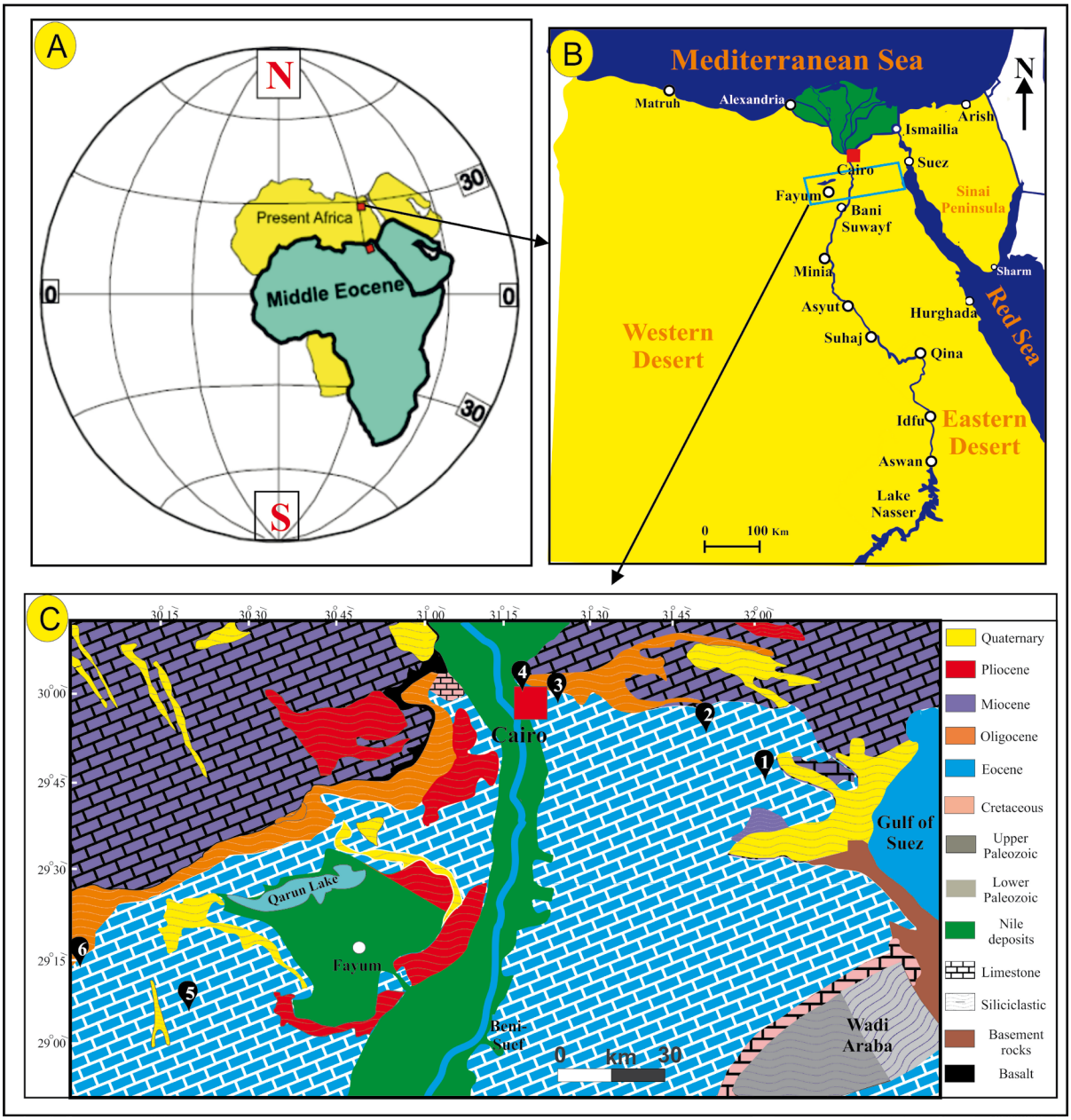

Figure 1. A- The Middle Eocene paleogeographic position of the African continent compared with the present day position of Africa. Modified from Lotfy and Voo (2007). B- Map of Egypt showing the location of the studied sections (area within rectangle). C- Geological map of the studied sections (1. Gebel el Ramliya, 2. Observatory, 3. Qattamiya, 4. Mokattam, 5. Minqar el Rayan, and 6. Wadi el Hitan sections).

Allam et al., 1991; Strougo et al., 1992; Boukhary et al., 1993; Omar, 1999; Mostafa and Hassan, 2004; Uhen, 2004; Lotfy and Voo, 2007; Abu Elghar, 2012, El-Fawal et al., 2013; Marzouk et al., 2014). The aims of this work are to document and interpret the sequences and diagenetic phases and to discuss possible relations between sequences and the diagenesis in the studied Middle Eocene strata in northern Egypt (Figure 1).

2. Geological setting

The studied sections exhibit good exposures of Middle Eocene rocks and are dominated by corals and foraminifers in the Gebel el Ramliya and Observatory sections. Bivalve shells and bryozoans in Cairo and sandstone, shale, and argillaceous limestone that is dominated by bivalve shells and foraminiferal shells, especially *Nummulites* spp., are seen in the lower part and only clastic sediments in the

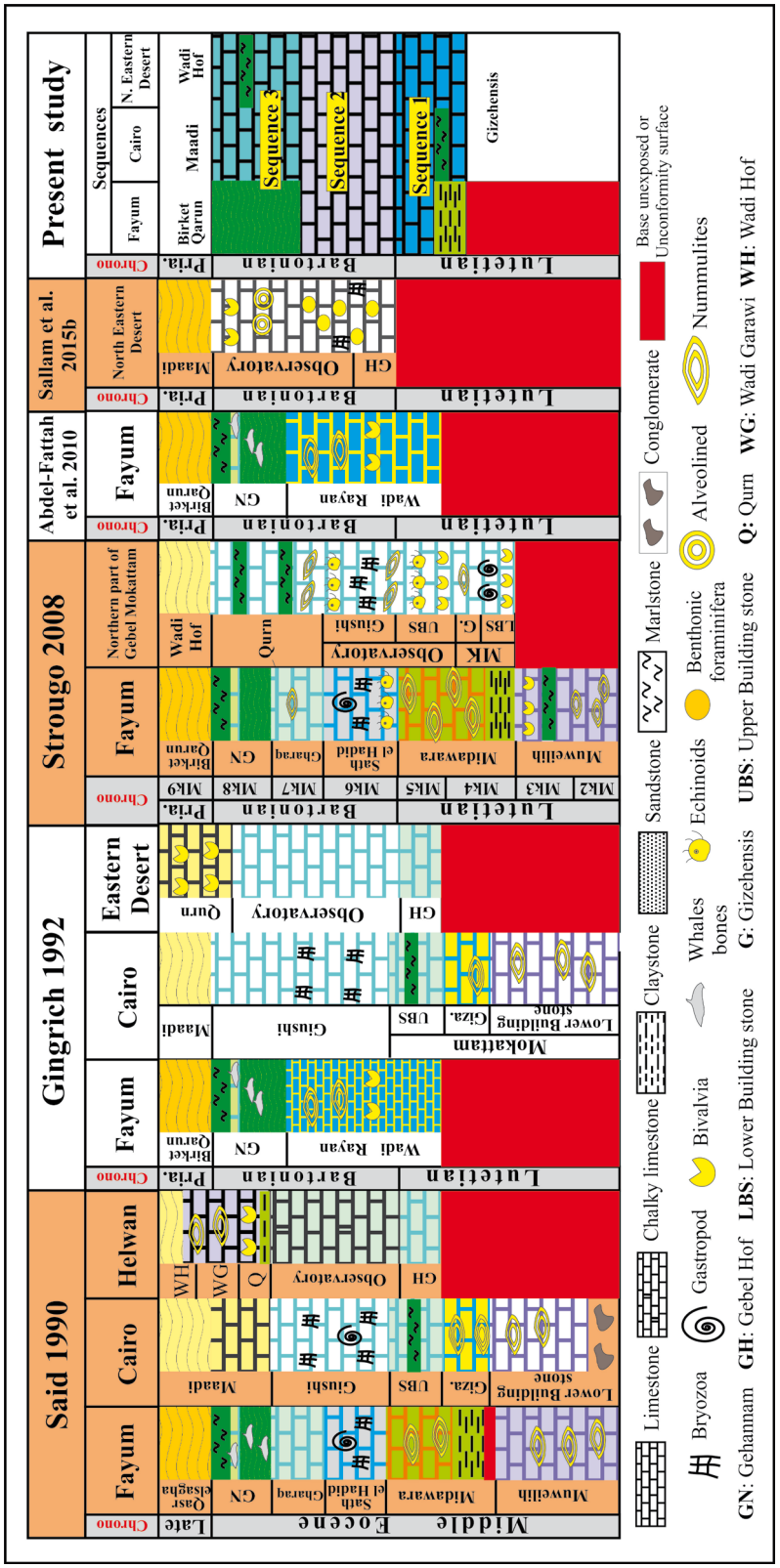

Figure 2. Comparison of previous main lithostratigraphic schemes showing the age assignments and lithostratigraphic nomenclatures of the Middle Eocene outcrops in Northern Egypt. No accurate scale for the lithostratigraphic units.

upper part. The Middle Eocene development of coral reefs at the Eastern Desert sections indicates the positioning of northern Egypt at a much lower latitude at such time than the present day. The growth of the corals should have occurred in a tropical to subtropical climate as confirmed by the paleomagnetic studies of the vertebrate sites in the North Western Desert (Lotfy and Voo, 2007). They located the placement of Egypt at 15°N to 17°N, particularly during the studied period (Figure 1). The geological history of the Egyptian Eocene was influenced by several tectonic events such as the Syrian Arc system, the Gulf of Suez rifting initiation, and the Alpine orogeny, which affected NE Africa and the Arabian platform as well. It resulted in crustal shortening and the inversion of sedimentary basins in the North Eastern Desert (Schandelmeier et al., 1997). Some of the distributions and nomenclatures of the Eocene rocks in Egypt are not established (Said, 1990). Lithostratigraphically, the studied Middle Eocene sections are characterized by different facies types due to sea-level changes and tectonic movements (e.g., Strougo 1985a, 1985b, 2008; Strougo and Boukhary, 1987; Helal, 1990, 2002; Said, 1990; Strougo and Abd-Allah, 1990; Strougo and Azab, 1991; Gingerich, 1992; Abdel-Fattah et al., 2010; Sallam 2015a, 2015b). The Fayum Facies includes the Wadi el Rayan and Gehannam formations; the Cairo Facies includes the Upper Building Stone and Giushi formations; and the North Eastern Desert Facies comprises Observatory and Qurn formations (Figure 2).

3. Methodology

Facies analysis, stratigraphic interpretation, and tracing of diagenesis features of the Middle Eocene sediments were carried out after a combination of field observations and petrographic investigations of six expressive localities in northern Egypt (Gebel el Ramliya (Gr), Observatory (Ob), Qattamiya (Qt), and Mokattam (Mk) in the Eastern Desert and Minqar el Rayan (Mr) and Wadi el Hitan (Wh) in the Western Desert) (Figure 1). The samples were collected with an interval of 0.2–1 m or 1–3 m in monotonous sequences. In each section, we examined and explored rocks, fossils, sorting, grains, structure, diagenesis, and other features. A total of 625 rock samples were collected from the field to produce 220 thin sections. These deposits were studied on site during the field trips with a hand lens and then classified according to the depositional fabric and lithofacies. A polarizing microscope was used to integrate lithological, paleontological, and diagenetic data for facies characterization and to construct the relation between diagenesis and sequence stratigraphy. The description and classification of these sequences depend on the following characteristics: carbonate textures, mineralogy, rock color, grain size, sorting, components (bioclastic or nonskeletal), thickness of the different rock units, bedding style, sedimentary features, authigenic mineralization, and diagenetic changes according to the classification of Embry and Klovan (1971). The sequence stratigraphic interpretations used in this study follow the approach and terminology of Embry et al. (1992), Emery and Myers (1996), and Kerans and Tinker (1997).

4. Results and discussion

4.1. Sedimentology

4.1.1. Lithofacies types

Twelve lithofacies types (LFTs) were identified in the studied Middle Eocene sections (Table 1; Figures 3–6). In general, the studied rocks are dominated by nummulitic banks carrying *Nummulites* spp. packed with other skeletal remains, poorly bedded and dolomitic in the lower Lutetian in all the studied sections. The upper Lutetian is characterized by fossiliferous limestone dominated by foraminifers and corals in the Eastern Desert sections, *Nummulites* spp. and echinoids in Cairo, and sandstones, shales, and argillaceous limestone beds in the Fayum (Figure 2). At the Bartonian, corals, molluscan shells, algae, and foraminifers dominate in the Eastern Desert sections; *Nummulites* spp., bryozoans, and bivalves prevail in Cairo; and marly and argillaceous fossiliferous limestones capped by clastic sediments belonging to the Wadi el Hitan section are dominant (Figure 2).

4.1.2. Lithofacies associations

Five lithofacies associations (LFAs) were distinguished in the studied sections depending on the grouping of LFTs (Table 2; Figure 3). Each LFA was given an interpretive name based on its position on the carbonate platform. These LFAs from east to west are reef core, back reef and outer lagoon, shoal, inner lagoon, and tidal flat.

4.1.3. Diagenesis

The series of Middle Eocene rocks are characterized by a progressive diagenetic sequence that influences the fossil record of the various biota. The diagenetic alteration in the studied sections is dependent on whether the primary microstructure and microarchitecture of the fossils are known. The variations in the fossil preservation can be linked to variations in sea level and the influence of meteoric diagenesis. The porosity in some LFAs decreases because of increasing cementation and micritization, and the dissolution is always followed by cementation. The internal properties of the studied fossils, such as microstructure, are key to understanding the rate of diagenetic alterations in the various studied LFAs. In this study, we determine the main diagenetic sequences on the scleractinian corals and foraminifers as follows.

4.1.3.1. Diagenetic sequence on the coral reef

Few authors have written about the progressive diagenetic sequence that influences the scleractinian corals (e.g.,

Table 1. The Middle Eocene lithofacies in northern Egypt.

LFT	Lithofacies and figures	Rock color and lithology	Sedimentary structures and diagenesis	Grain size and sorting	Main components	Thickness	Environment and interpretation
Tidal flat	Clastic rocks Figures 4a and 4b	Gray, yellow, yellowish white, brown Cs and Ss	Fissile, joints, roots, carbonized, burrows, silicification	Fine to coarse, moderately to well sorted	Rare shells, gypsum veins whale bones	Several dm to m	Gypsum, vertebrate fossils, and clastic rocks indicate tidal flat to near shore environment (Gingerich, 1992)
	Dolomudstone Figure 4c	Gray to white, yellow dolo Ls	Lamination, bioturbation, dolomitization	Siltite to lutite, moderately sorted	Qz grains, rare bioclasts	dm	Rare fossils and dolomite rhombs indicate tidal flat deposits
Inner lagoon	Bioclastic foram. wackestone Figure 4d	Yellowish white to pale yellow Ls and Dl	Cross and flaser bedding, burrows, micritization, cementation	Lutite to arenite, moderately to poorly sorted	Miliolids, algae, rotaliids, bivalves, peloids	Several dm	The plentiful miliolids, peloids, and the mud texture show restricted to inner lagoon environment
	Bioclastic foram. Wacke- to packstone Figures 4e and 4f	White to yellowish white argillaceous limestone	Planer and cross bedding, leaching, cementation	Siltite to arenite, poorly to well sorted	*Nummulites* spp., bivalves, peloids echinoids,	Several dm to m	Low to moderately agitated shallow water below FWWB in the upper subtidal regime (El-Azabi, 2006)
	Foram. bivalvian wacke- to floatstone Figures 4g and 4h	Yellow to grayish white argillaceous and marly Ls	Laminated and thinly bedded, micritization, dissolution	Siltite to arenite, ill to well sorted	Oyster shells, foram., gastropod, algae	dm	The abundance of oysters and other bioclasts indicates lower intertidal to subtidal site of a quiet-water shelf lagoon
Shoal	Aggregate grains, grain- to rudstone Figure 5a	Gray to white, Ls and Dl	Unbedded, fractures, micritization, compaction, cementation,	Rudite, moderately to well sorted	Lithoclasts, foram., bivalves, peloids, echinoids	dm	Lumps, micritization, and peloids indicate restricted to open shelf in the inner lagoon to shoal setting
	Bioclastic foram. grainstone Figures 5b and 5c	White to yellowish white Ls and chalky Ls	Cross-laminated to planar, micritization, cementation	Rudite, moderately to well sorted	*Nummulites*, coral, alveolinids, peloids, echinoid spines	dm to m	This texture has been deposited in moderate to high energy above NWB at the shoal setting
Outer lagoon and back reef	Nummulite echinoid wackestone Figures 5d and 5e	Yellowish white to gray argillaceous Ls and Ls	Thinly to thick-bedded, micritization, aggrading neomorphism	Rudite, moderately sorted	*Schizaster* sp., *Nummulites*, foram., bivalves	Several meters	According to Flügel (2010), echinoid facies indicate subtidal setting in an outer lagoon environment
	Bioclastic bryozoan wacke- to floatstone Figures 5f and 5g	Grayish white to white argillaceous Ls and Ls	Planar and cross-lamination, intraparticle porosity	Rudite to arenite, moderately to poorly sorted	*Tremogastriona* sp., *Nummulites* sp., bivalves	Several meters	The plentiful big-sized bryozoans indicate low energy, quiet lagoon under NWB (Ziko, 1985)
	Bioclastic coralline floatstone Figures 5h and 6a	Yellowish white to yellow marly Ls and dolostone	Bedded, branching, elliptical shape corals, cementation	Rudite to arenite, moderately to poorly sorted	*Goniopora* sp., foram., echinoids, bivalves	dm to m	The shape of corals and the presence of *Goniopora* sp. and other bioclasts refer to back reef setting (Bruggemann et al., 2004)
Reef core	Bioclastic coralline pack- to rudstone Figures 6b and 6c	Grayish white, yellowish white Ls and Ds	Cavernous, unbedded, micritization, aggrading neomorphism	Rudite to siltite, poorly sorted	Corals, coralline algae, foram., echinoids	Several meters	The facies indicates reef setting and the presence of other bioclasts signfies some transportation (Nichols, 1999)
	Bioclastic coralline boundstone Figures 6d and 6e	Brownish yellow to yellowish white Ls and marly Ls	Fractured, massive, leaching, neomorphism, recrystallization	Rudite to arenite, moderately to poorly sorted	Corals, alveolinids, miliolids, echinoids, bivalves	dm to m	The density and the abundance of coral boundstones indicate reef flat and crest in the reef setting (Shen et al., 2008)

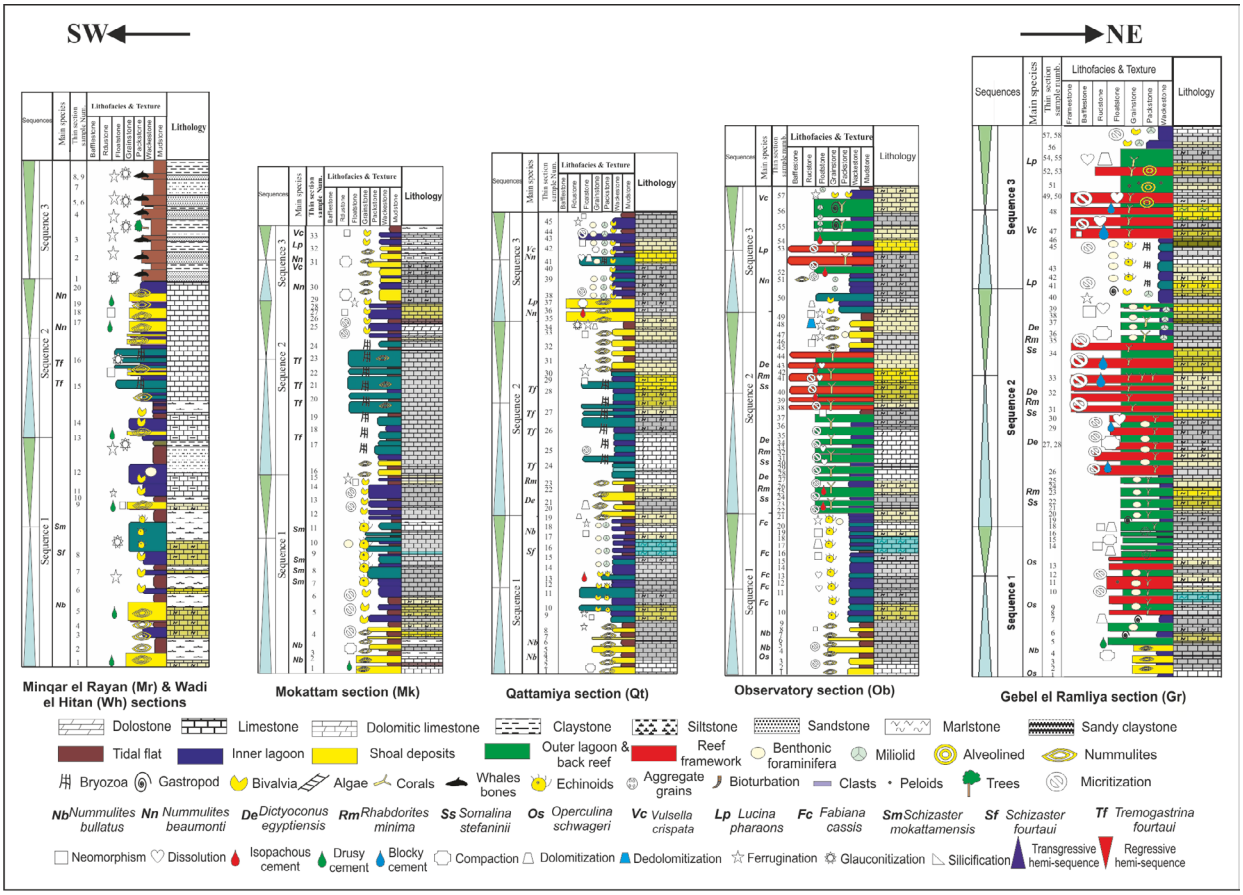

Figure 3. The relationship between diagenetic features and the sequence stratigraphy at the studied section.

Gvirtzman and Friedman, 1977; Dulo, 1986; Nothdurft and Webb, 2009; Johannesson, 2012; Van Woesik et al., 2013). The changes of coral frameworks are interrelated and collectively constitute the sequence of progressive diagenesis. The aragonitic framework secreted by the living tissue of the scleractinians shows only a rare cementation. Most of the pores are interskeletal separate voids. With progressive diagenesis, the organic matter decomposes and the separate pores become connected. The outer parts of the skeletons become lined with micrite envelopes (Figure 7a), which is followed by the first marine cementation phase. The scleractinians are fringed by isopachous fibrous cement and consist of rods and needles of aragonite. These two types of cement may occur separately or together in the marine phreatic environment (no aragonite cement appeared in the studied sections because it is completely dissolved or recrystallized to calcite in the meteoric waters).

Dissolution of aragonite is common and has effects on corals and aragonite sediment (Figures 7b and 7c). The aragonite of the coral framework is stable under marine conditions, but under the influence of subaerial conditions and mixing with meteoric water, it becomes unstable and tends to change into a stable mineral (low Mg-calcite). The vugs resulting from leached corals are partly filled with neomorphic and blocky calcite, which may grow instead of dissolved aragonite needles (Figure 7d). The second marine cementation phase, prismatic (Figure 7a), and blade-like calcite crystals are detected in some thin sections, where they form linings to open pores. The form of these crystals is acute scalenohedral 'dog tooth' (Figure 7e), or obtuse-angled rhombohedral 'nail head' (Figure 7f) with plane and harmonious terminations between crystals (Figure 7f). Braithwaite and Montaggioni (2009) stated that morphological variations in crystal are related to changes in the crystal growth rates, water chemistry, and the combined factor of the relationship between sea-level variation and the Paleo-water table. Although many authors interpreted the dog tooth as a result of meteoric influence (e.g., Wallace et. al., 1991; Koch and Zinkernagel, 1996), the marine source of the dog tooth cement is incontrovertible as documented in several papers (Strasser and Stohmenger, 1997; Reinhold, 1999; Braun, 2003). Palermo (2008) reported that the nonappearance of a sharp boundary between dog tooth cement in addition to the similarity in color and harmonious terminations as

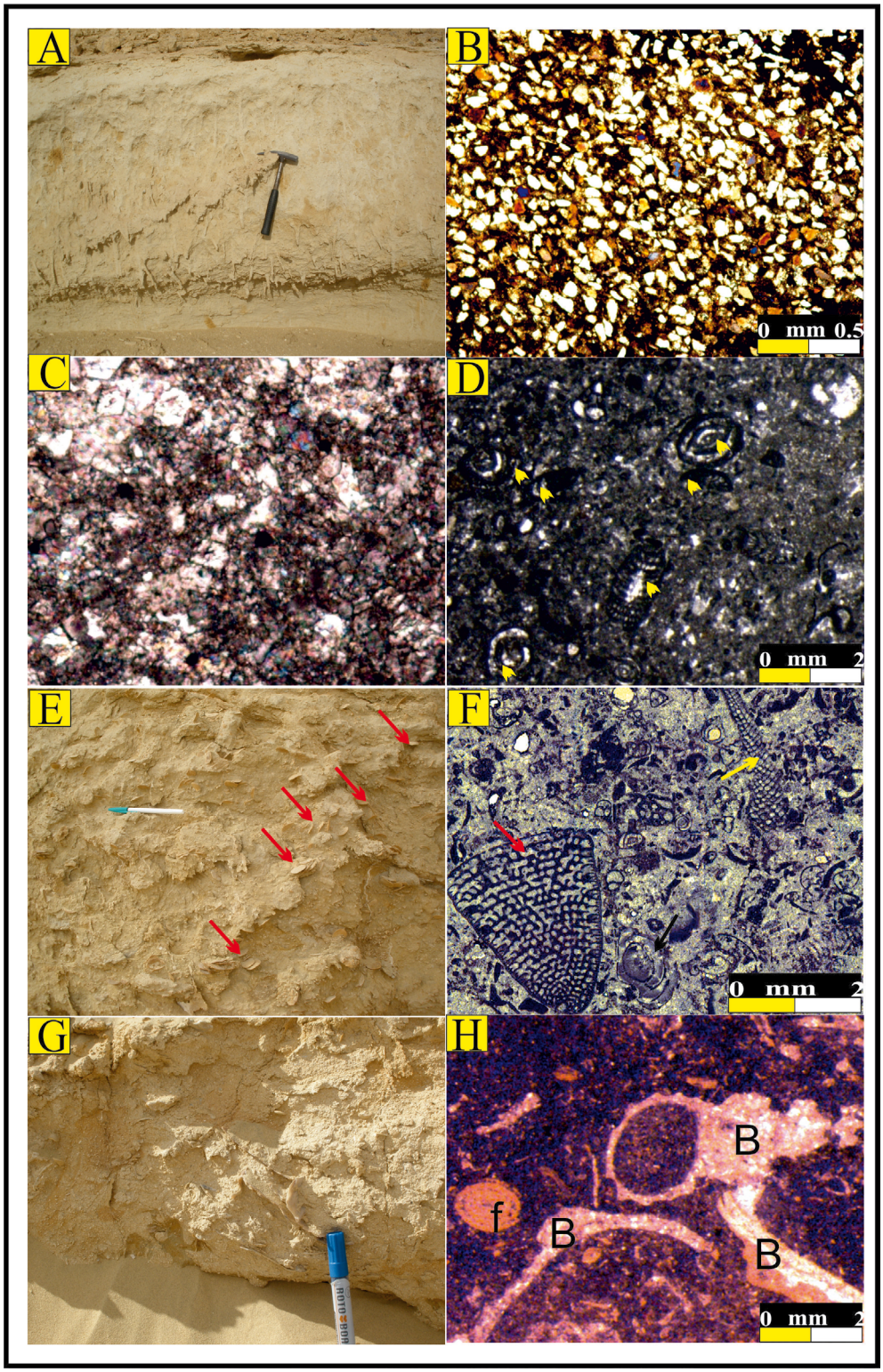

Figure 4. Outcrop photographs and thin section photomicrographs. A- Root casts embedded in the sandstone bed, Wadi el Hitan section, sample number (Sn): Wh5. B- Ferruginous bioclastic arenite contains some glauconite grains, Sn: Wh8. C- Dolomudstone dominated by dolomite grains, Qattamiya section, Sn: Qt19. D- Bioclastic wackestone contains many different foraminiferal species (arrows), Observatory section, Sn: Ob20. E- Marly limestone consists mainly of *Nummulites* spp. (arrows), Minqar el Rayan section, Sn: Mr5. F- Foraminiferal wacke- to packstone consists of *Dictyoconus egyptiensis* (red arrow), *Idalina* sp. (yellow arrow), *Rhabdorites* (yellow arrow), and others, Observatory section, Sn: Ob47. G- Different types of bivalve shells, Minqar el Rayan section, Sn: Mr17. H- Foraminiferal (F) bivalve (b) wacke- to floatstone, Minqar el Rayan section, Sn: Mr12.

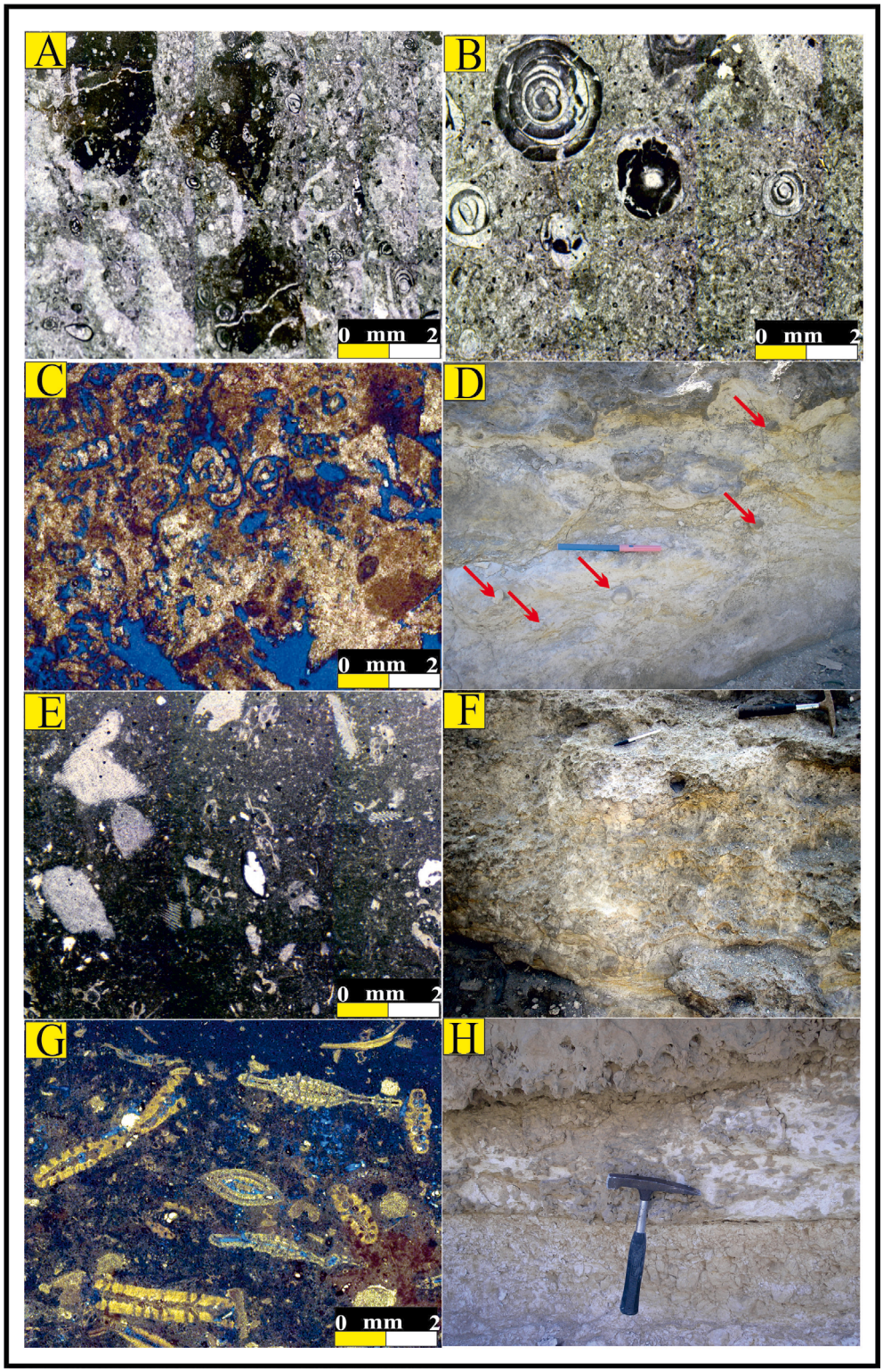

Figure 5. Outcrop photographs and thin section photomicrographs. A- Aggregate grains and lithoclasts grain- to rudstone, Gebel el Ramliya section, Sn: Gr16. B- Bioclastic peloidal grainstone consists mainly of different types of *Alveolina* sp. and peloids, Gebel el Ramliya section, Sn: Gr51. C- Inter- and intraparticle porosities in the bioclastic grainstone texture, Gebel el Ramliya section, Sn: Gr51. D- Infaunal echinoid burrows in the limestone beds, Mokattam section. E- Foraminiferal echinoid wackestone consists mainly of echinoid grains and spines, Mokattam section, Sn: Mk10. F- Bryozoan beds dominated by *Tremogastrina fourtaui*, Mokattam section, Sn: Mk24. G- *Nummulites* bryozoan wacke- to floatstone, Mokattam section, Sn: Mk23. H- Broken, irregularly arranged small fragments of branching corals over the wackestone beds, Gebel el Ramliya section, Sn: Gr44.

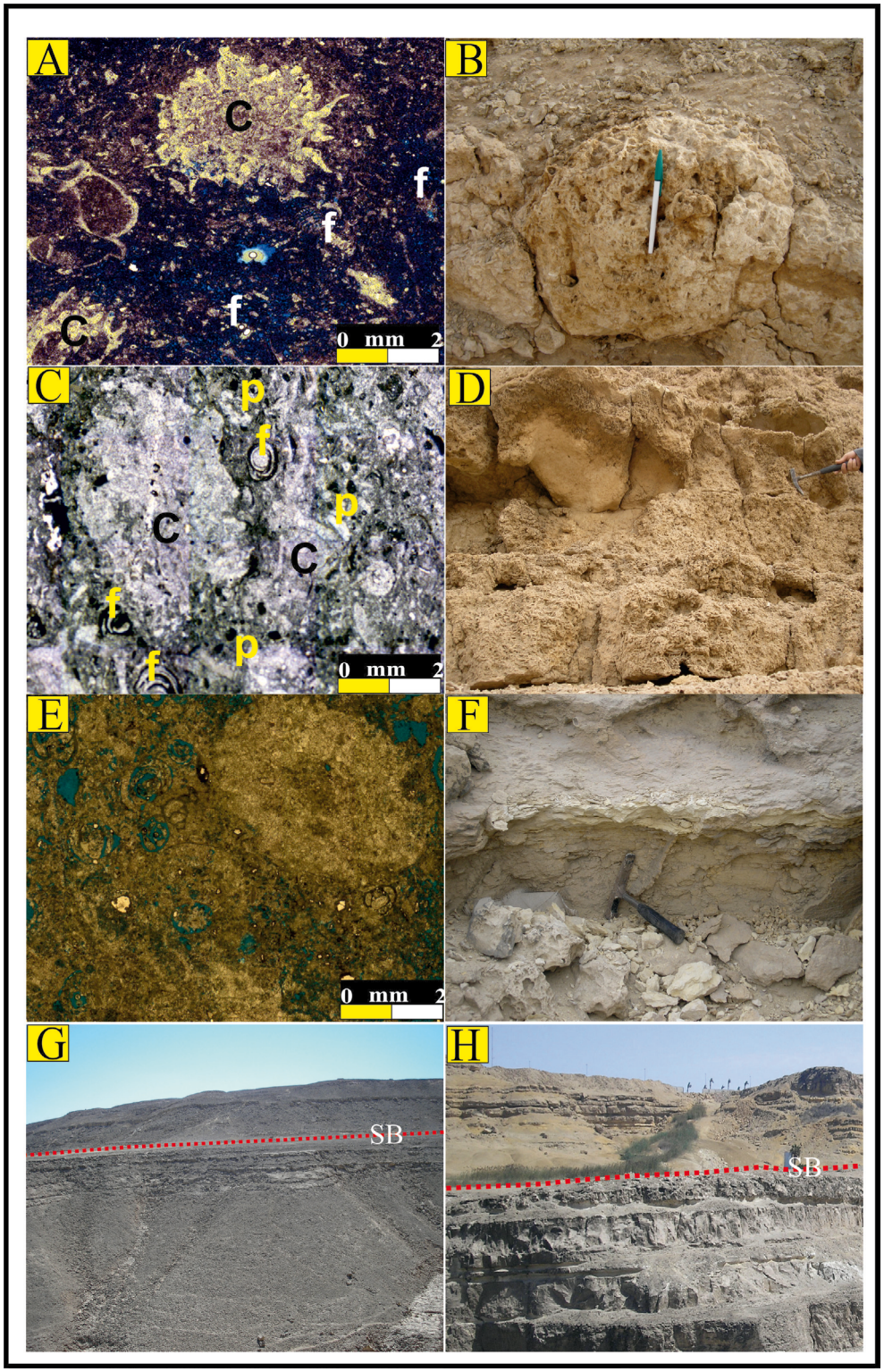

Figure 6. Outcrop photographs and thin section photomicrographs. A- Bioclastic coralline floatstone dominated by corals (c) and foraminifera (f), Gebel el Ramliya section, Sn: Gr25. B- Cavernous, fractured, and unbedded coralline limestone, Gebel el Ramliya section. C- Bioclastic coralline pack- to rudstone consists of coral grains (c), peloids (p), and foraminiferal tests (f), Gebel el Ramliya section, Sn: Gr11. D- Numerous broken branching corals at the transgressive part, Gebel el Ramliya section. E- Bioclastic coralline framestone, Gebel el Ramliya section, Sn: Gr33. F- Gypsiferous claystone at the top of Sequence 1, Qattamiya section. G- Sequence boundary (SB) between S2 and S3 at the Observatory section. H- Sequence boundary (SB) between the Middle Eocene carbonate rocks (S3) and the Upper Eocene sandstone rocks at the Mokattam section.

Table 2. The Middle Eocene lithofacies associations in northern Egypt.

Lithofacies association	Sedimentary features	Depositional environment
LFA 1: Tidal flat	Consists mainly of major clastic rocks (claystone, siltstone, and sandstone) and minor mudstones. Gypsum veins and halite crusts are common. Iron traces and glauconitization are recorded in the clastic rocks. Whale bones and rare shell hash are obvious in the studied sections	The presence of shell fragments and clastics without distinguished lamination indicates low energy tidal flat in arid climate (Zonneveld et al., 2001; Sedgwick and Davis, 2003).
LFA 2: Inner lagoon	Siltite, arenite and lutite wackestone, packstone, and floatstone. Poorly to moderately sorted. Cross and flaser beddings are recorded. The main fossils are bivalves, gastropods, algae, and foraminifers, especially miliolids, *Nummulites* spp., and Textulariida, with lithoclasts, aggregate grains, and peloids. Small percentage of clastic rocks is present. Micritization, recrystallization, and dolomitization are the main diagenetic features.	The presence of miliolids and other bioclasts indicates low energy, restricted to open marine water below FWWB (Adabi et al., 2008). The existence of aggregates and some detrital material signifies some reworking and transportation.
LFA 3: Shoal deposits	Arenite, lutite and rudite packstone, grainstone, and rudstone. Moderately to well sorted. Imbrication and cross bedding are common. The main fossils are *Nummulites* spp., alveolinids, oyster shells, and algae. The main diagenetic features are drusy cement, micritization, and leaching.	The presence of *Nummulites* grainstone indicates high energy conditions with open circulation (El Ayyat, 2013) and according to Kovacs (2005) the existence of oysters corresponding to *Nummulites* indicates water depth near the FWWB.
LFA 4: Outer lagoon and back reef	Siltite, arenite, lutite and rudite wackestone, floatstone, and rudstone. Poorly to moderately sorted. Cavernous and unbedded coralline rudstone. Bryozoans, echinoids in life position, bivalves, and corals are the main fossils. Aggrading neomorphism, cementation micritization, partial dolomitization, and interparticle and intraparticle porosities are the common diagenetic features.	Echinoid and bryozoan beds in the studied sections indicate low energy outer lagoon environment behind the reef framework setting (Tawfik et al., 2016). The development of coral rudstone and floatstone signifies back reef behind the reef core (Cabioch et al., 2008).
LFA 5: Reef core	Arenite and rudite boundstone. Poorly to well sorted. Corals, foraminifers, and algae are the main bioclasts. The coral beds are massive and bedded. Aggrading neomorphism and micritization are the common diagenetic features.	The abundance of hermatypic corals and the development of massive and dense coral framestone indicates a reef crest (Shen et al., 2008).

in the current studied thin sections refers to the marine origin of the dog tooth cement.

4.1.3.2. Diagenetic sequence on the foraminiferal tests

The foraminiferal tests occur mainly in shoal and lagoon LFAs, which comprise grain- to packstones, interbedded with wackestones. Foraminiferal tests in these beds are dominated by *Nummulites* sp. and alveolinids and most tests of the foraminifera are calcitic. The tests are influenced by the micritization that forms micrite envelopes. These envelopes form within the marine phreatic environment (Flügel, 2004) and have different thicknesses (Figure 8a). The micritization process is followed by three types of marine cementation; the first marine cementation is fringed by bladed and needle-shaped calcite isopachous fibrous cement, which is indicative of a marine phreatic environment. This cementation prevents extensive compaction and partly occludes interparticle pores (which are not clearly apparent as a result of bad preservation). This type of cementation is followed by leaching, where large portions of the foraminiferal grains are affected by selective dissolution. This dissolution process is generally considered to be caused either by subaerial exposure and/or fresh water influence under shallow water conditions. This phase is responsible for the vuggy, moldic, intergranular, and intragranular porosities (Flügel, 2004) observed in these LFAs. The leaching phase results in a large increase in porosity, but permeability is low with separate vug porosity only (Figure 8b). The second marine cementation is observed on a minor scale, in the form of isopachous fringe cement inside dissolved skeletal components. This cement is responsible for a decrease in separate moldic porosity (Figure 8c). The last type of marine cementation is a drusy and granular calcite spar of this final cementation phase, which is widespread,

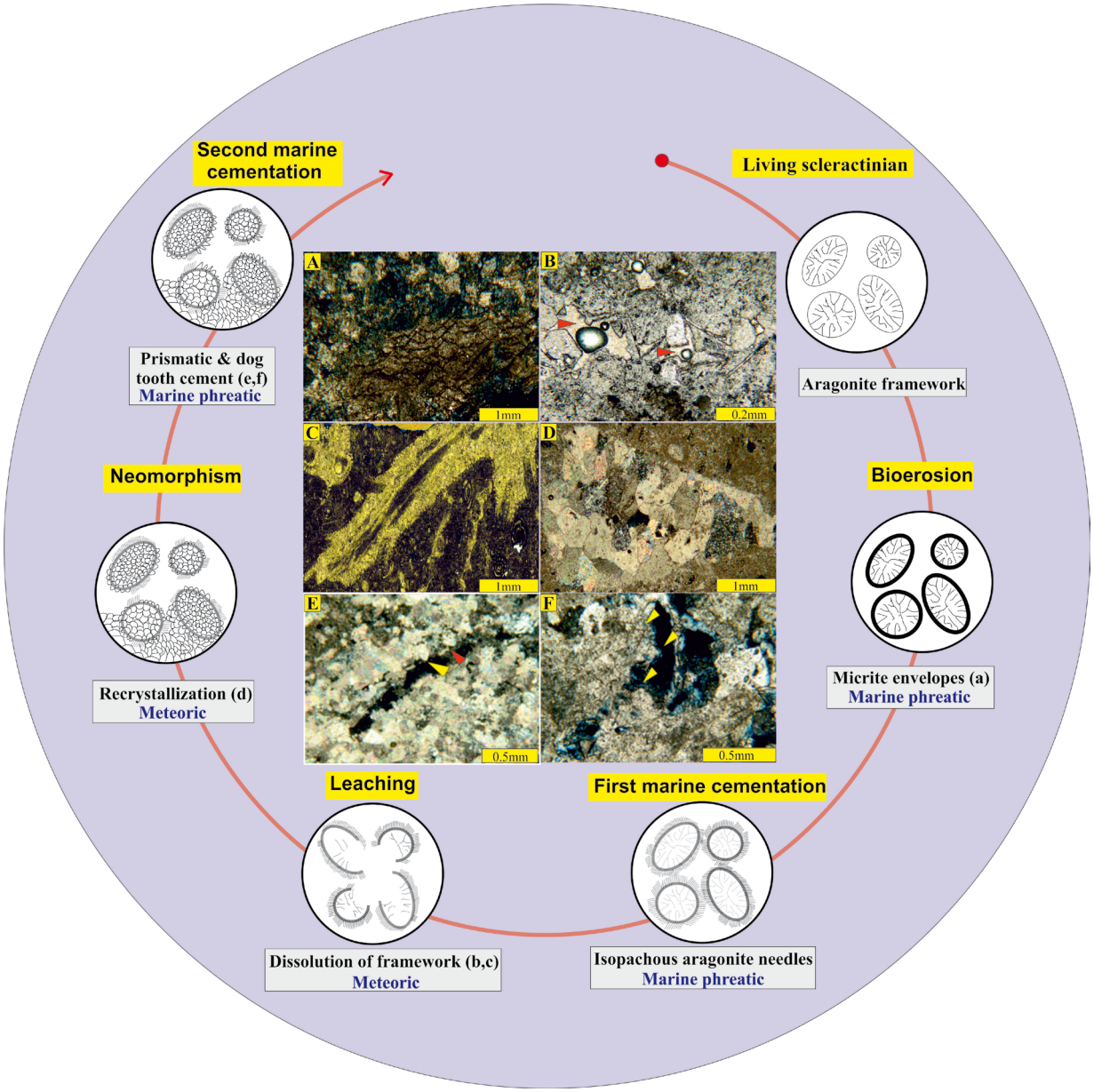

Figure 7. Schematic figure illustrates the effect of the diagenetic sequence in a coral framework and thin section photomicrographs: a- Prismatic crystals of crystallized calcite. Note the micritization in the colony, S1, Sn: Gr11. b- Selective dissolution in the coral framework (red arrow). The voids are filled with blocky calcite, S3, Sn: Gr47. c- Leached corals, filled with internal sediment, S3, Sn: Gr49. d- Neomorphized coral skeleton, S3, Sn: Gr48. e- Neomorphized calcite crystals with dog teeth termination (no clear dog tooth crystals arrow), S2, Sn: Gr33. f- Neomorphized calcite crystals with a nail head (yellow arrow) and a flattened concordant termination (red arrow), S2, Sn: Gr34. Note: All photos from the Gebel el Ramliya section.

especially in *Nummulites* sp. beds. The anhedral to subhedral nonferroan calcite crystals fill the void and pore lining cement in intergranular and intraskeletal pores, molds, and fractures in a meteoric environment. Due to the increasing crystal size this cement is the most important pore-filling, porosity-destructive cement. Both interparticle and moldic pores are greatly reduced by coarse equant calcite spar (Figure 8d). After the cementation, many foraminiferal tests are influenced by compaction, dolomitization, dedolomitization, silicification, glauconitization, and ferrugination. The compaction is subjected to only shallow burial. Mechanical compaction results in a closer packing of foraminiferal tests, and fracturing and fragmentation are common (Figure 8e).

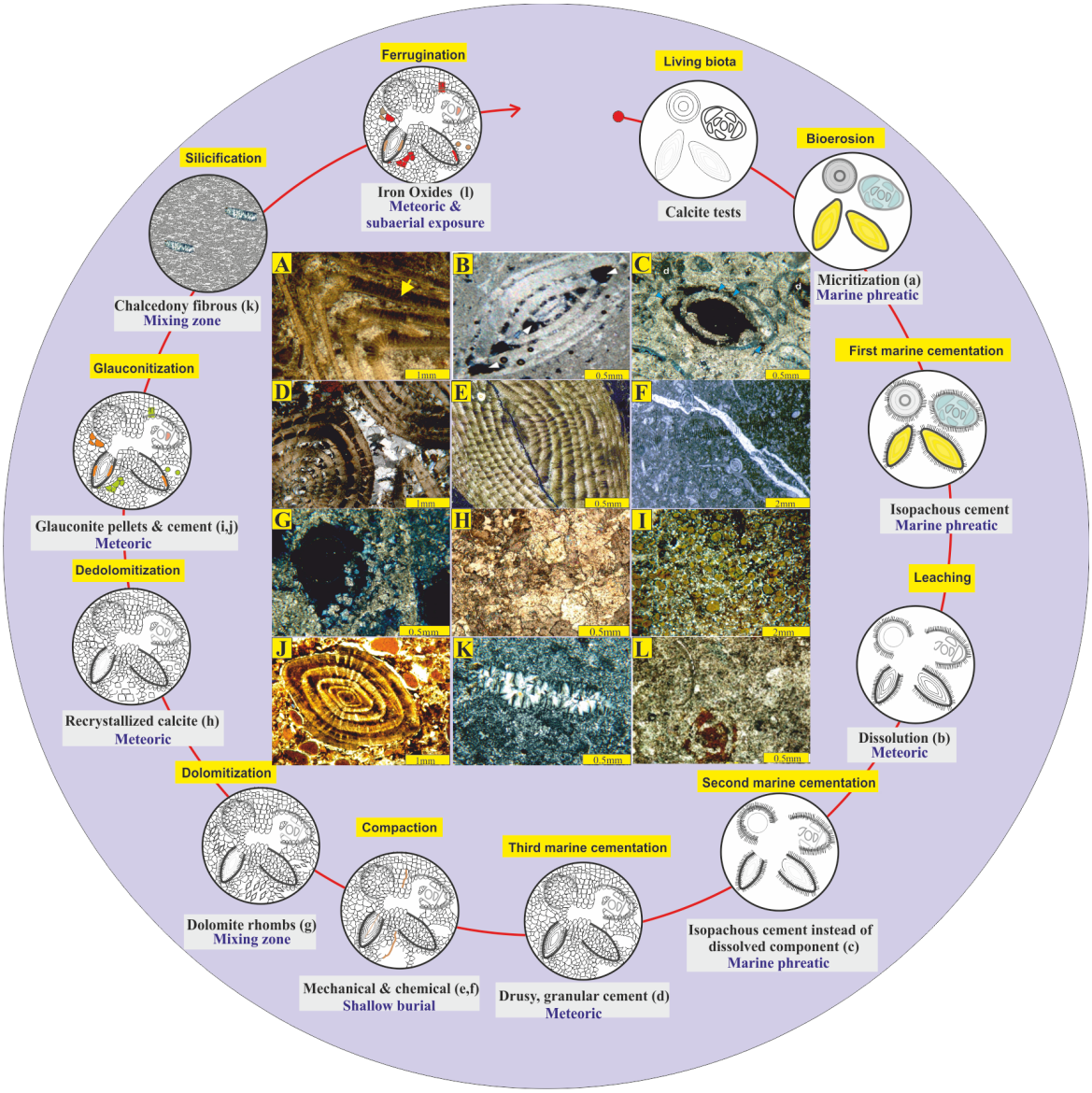

Figure 8. Schematic figure illustrates the effect of diagenetic sequence in foraminiferal tests and thin section photomicrographs: a- Micritization (yellow arrow) in *Nummulites* test. Notice that the test consists of a thick wall that has a radial fibrous structure. S3, Qattamiya section, Sn: Qt43. b- Moldic pores formed by dissolution of bioclasts in microcrystalline calcite (white arrow). S2, Qattamiya section, Sn: Qt40. c- Second marine cementation isopachous fringe cement (blue arrow) precipitated after the large-scale dissolution phase. S1, Qattamiya section, Sn: Qt5. d- *Nummulites* grainstone pervasively cemented by drusy and granular meteoric low-Mg calcite after fibrous rims. S2, Minqar el Rayan section, Sn: Mr9. e- Mechanical compaction (fracture) on the *Nummulites* test. S3, Qattamiya section, Sn: Qt37. f- Crosscutting straight to arched fractures filled with calcite 'veins'. S2, Gebel el Ramliya section, Sn: Qt42. g- Dolomite crystals lining vuggy pores in partially dolomitized intraclastic grainstone. S2, Observatory section, Sn: Ob46. h- Structureless dedolomites. S2, Gebel el Ramliya section, Sn: Gr39. i- Glauconite aggregates, rounded to subrounded. S2, Wadi el Hitan section, Sn: Wh5. j- Glauconite cement replaces micrite that fills the chambers of the *Nummulites*. S2, Minqar el Rayan section, Sn: Mr16. k- Radially fibrous chalcedony on a bioclastic shell. S3, Wadi el Hitan section, Sn: Wh4. l- Iron oxides on a foraminiferal test. S1, Mokattam section, Sn: Mk15.

In contrast, chemical compaction is not common and is observed in the formation of stylolites and solution seams (Figure 8f). Many fractures are filled with iron oxides and sparry calcites. Compaction is responsible for the reduction of the inter- and intracrystalline porosities. In some foraminiferal tests, the dolomite grains partially to completely replace the limestone matrix and selectively replace bioclastic grains. The dolomite rhombs in the

bioclastic grains are euhedral to subhedral and no zoning was observed in individual rhombs. Dark rhomb cores and clear rims are common. Holiel (1994) pointed out that the presence of these dolomite grains in the Middle Eocene suggests dolomite precipitation from progressively less saline water, resulting from the mixing of freshwater and seawater (Figure 8g). Dedolomitization is also recorded as completely recrystallized calcitic rocks showing a highly variable appearance under the meteoric conditions. The dedolomitized grains in the studied sections have different crystal sizes and always correspond to ferrugination (Figure 8h). The origin of dedolomitization may be related to the metastability of the ferroan dolomites in the mixing zone under surface status. The spreading of phreatic or meteoric water is responsible for the hydration and oxidation of the ferrous iron content of the ferroan dolomite. In the Qattamiya and the Minqar el Rayan sections, glauconitic minerals are reported in the rocks, especially in the argillaceous limestones and claystones. The glauconites are formed either as cement or by the diagenetic alteration of host minerals like quartz, feldspar, and calcite minerals within the meteoric environment. The glauconites occur as aggregates (Figure 8i) that are granular, rounded to subrounded, moderately sorted with elliptical outlines, and with a smooth surface texture. Some skeletal fragments show complete replacement of their structures by the glauconites. Some of the glauconites are autochthonous and fill the structures of the skeletal particles and others are allochthonous. It is noticed from the petrographic investigation that these glauconites are formed by the replacement of the clay minerals that were trapped within the fossil tests (such as *Nummulites* sp. chambers) (Figure 8j). Abu Elghar and Hussein (2005) stated that the glauconitization process in the Eocene is achieved by the addition of iron to the clay minerals to form glauconite by iron exchange processes favored by slightly reducing conditions, free access of seawater, and a pH at around 8. In the studied carbonate sections, the source of iron minerals is attributed to hydrothermal fluid accompanied with post-Middle Eocene volcanic activities, which increased the iron concentration. The presence of bacterial action increases the rate of reducing conditions, which clean out oxygen and increase the number of hydrogen ions as free radicals, which increase the total alkalinity of the succession in the phreatic-meteoric conditions.

Silicification in the Middle Eocene may be described as a later diagenetic process, which occurred under meteoric phreatic diagenesis and has been proven at the Qattamiya, Minqar el Rayan, and Wadi el Hitan sections corresponding to fractures and leaching. This process occurs when the initial silica replacement in the tests and shells of bioclasts such as *Nummulites* sp. and bivalves was done by length-fast fibrous chalcedony. The fast chalcedony (Figure 8k) also occurs as fringing cement-rimming bioclasts. The chalcedony was formed by the dissolving of Mg^{2+} from the dolomite (Hesse, 1988). Iron is available in the sediments of the Minqar el Rayan as pyrite minerals (FeS_2) (Figure 8l). Some traces of a ferruginous pigment are recorded on the tests and in cements as patches of iron oxides with red and brown crystals of microspar grains. This process may be related to subaerial weathering that leads to the formation of goethite and hematite under the effect of oxidation or of hydrothermal solutions rich in iron associated with volcanic activity.

4.2. Sequence stratigraphy

Although the general stratigraphy of the Middle Eocene has been described and examined by many authors, the sequence stratigraphy of the studied sections has been examined by only a few of them, such as El-Azabi (2006), Abu Elghar (2012), El-Fawal et al. (2013), and Tawfik et al. (2016). El-Azabi (2006) discussed the sequence stratigraphy of the Middle Eocene sequences in the North Eastern Desert and he determined three sequences in the studied sections. Abu Elghar (2012) divided the Middle Eocene studied sections in the Fayum area in the Western Desert into four sequences: sequence 1 equals the Samalut Formation (lower Lutetian); sequence 2 equals the El Muwelih Formation (upper Lutetian); sequence 3 equals the Midawara, Sath el Hadid, and Gharaq formations (lower Bartonian); and sequence 4 equals the Gehannam Formation. The two previous studies' results match our works on the Middle Eocene.

In general, the studied depositional sequences show various LFTs that enable us to compare them with the global eustatic sea-level curve of Haq et al. (1987). This comparison reflects the remarkable match between the present work's sea-level curve and that of Haq et al. (1987) during the Middle Eocene period (Figure 9).

4.2.1. Sequence boundaries

Catuneanu et al. (2009) claimed that sequences are formed due to changes in eustatic sea-level and/or tectonic activities. The studied sequences demonstrate that the origin of their boundaries are related to eustatic sea-level fluctuation rather than tectonic movements. The explanation of the sequence stratigraphy of the Middle Eocene successions is used to clarify the vertical and lateral lithofacies changes and to define the sequence boundaries and their links to eustatic sea level. Extensive studies of the collected rocks and fossils enable us to define four sequence boundaries (SBs) on top of the regressive parts in all of the studied sections (Table 3). These sequence boundaries mark three third-order sequences. SB1 lies between the studied sections and the underlying sections. The base of this sequence in the Eastern Desert and in the studied sections of Cairo is marked by changing from *Nummulites gizehensis* beds to other *Nummulites* spp. such

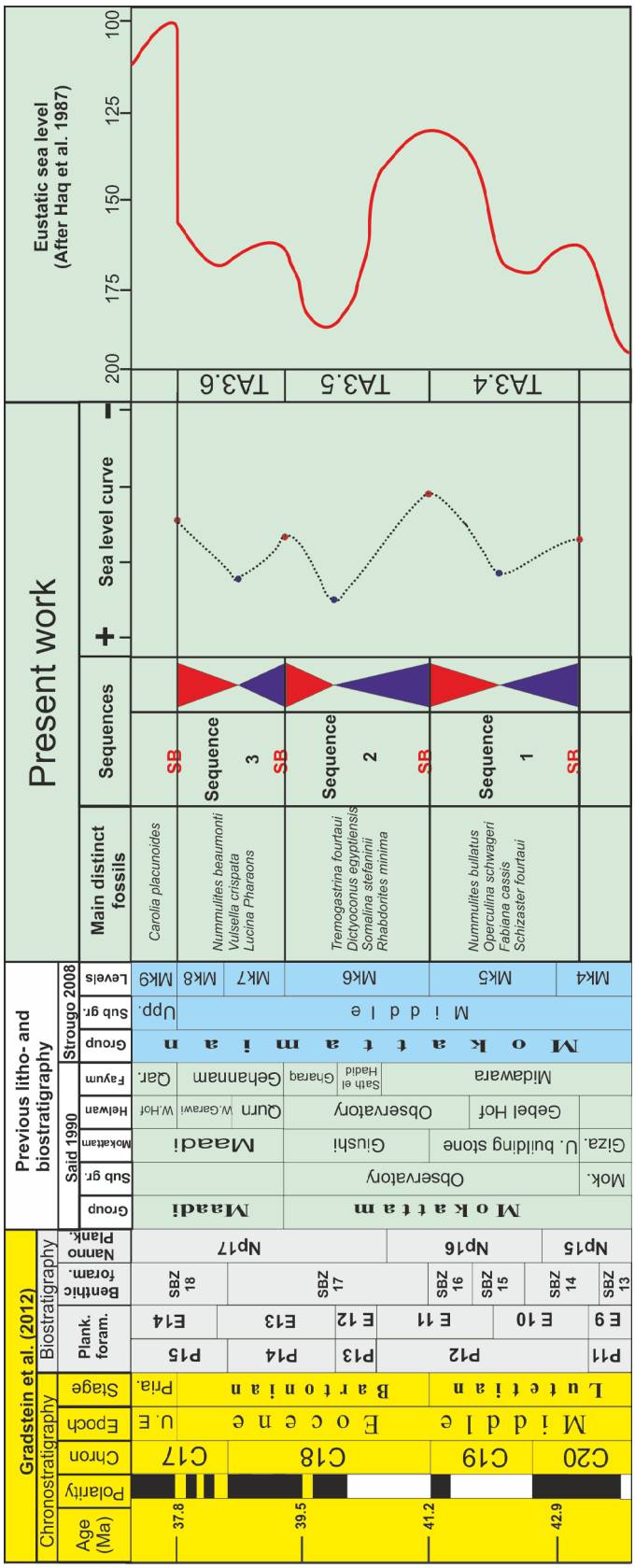

Figure 9. The correlation chart of the lithostratigraphy shows identified sequences and sequence boundaries of the stack of the studied Middle Eocene sections compared with the chrono- and biostratigraphy of Gradstein et al. (2012) and the global eustatic sea-level curve of Haq et al. (1987).

Table 3. The Middle Eocene sequences in northern Egypt.

S.	Seq. str.	Lithology	Lithofacies	Corresponding fossils	Sedimentary structure and diagenesis	Depositional environment
Sequence 1	TST1 (Figures 4d, 4e, 6b, 6c)	Claystone at Mr, limestone, marly Ls	- Bioclastic wacke- to mudstone. - *Nummulites* wacke- to packstone	*Nummulites* sp., *N. gizehenesis* at Mr; *N. praestriatus* and *N. bullatus* at Mk, Qt, Ob; other foraminiferal spp. at Gr	Thin-bedded, recrystallization, dog tooth cement, interparticle and intraparticle porosities	Inner lagoon to shoal
	MFZ (Figures 5d and 5e)	Marly Ls and Ls	- *N.* echinoid wackestone - *N.* bivalve wacke- to packstone at Mr, Mk, Qt, and Ob. - Bioclastic coral. floatstone at Gr.	Echinoids such as *Schizaster mokattamensis*, *Fibularia* sp., bivalve shells (*Fimbria* sp.), and larger foraminifera at MR, MK, Qt, Ob; corals such as *Goniopora* sp. at Gr	Laminated to thinly bedded, imbrications, glauconitization, interparticle and intraparticle porosities	Outer lagoon and back reef
	HST1 (Figure 5a)	Ls and Dl	- Bioclastic wackestones at Mr, Mk - Bioclastic wacke- to floatstone at Qt, Ob, Gr	Bivalve casts and gastropods at Mr, Mk; foraminifera and shell accumulations at Qt, Ob, Gr	Flaser bedded, coated grains, irregular pseudospar patches, dolomitization and vuggy porosity	Inner lagoon
	SB (Figures 4c and 6f)	Gypsiferous Cs at Mr, Mk, Qt, and Ls	- Lime mudstone at Ob - Congl. pebbles of mudstone at Gr	Miliolids, gastropods, algae	Sharp contact, ferrugination	Tidal flat
Sequence 2	TST2 (Figure 5f–5h and 6a)	Ls and marly Ls	- Molluscan wacke- to packstone - Bioclastic coralline floatstone at Gr	Bivalve shells, gastropods, foraminifera; foraminifera and corals such as *Astroconia* sp., *Stylophora* sp. at Ob, Gr	Cross- to planar-bedded, massive, isopachous cement, aggrading neomorphism	Inner lagoon, back reef
	MFZ (Figures 6d and 6e)	Marly Ls and Ls	- *N.* bryozoan wacke- to floatstone - Foraminiferal coral, boundstone at Ob, Gr	Bryozoans such as *Tremogastrina fourtaui* at MR, MK; *Membranipora* sp., *Steiginoporella* sp., *Nellia* sp. at Qt; echinoids and corals at Ob, Gr	Wedge-shaped and cross-bedded, acicular cementation, glauconitization, interparticle and intraparticle porosities	Outer lagoon and reef framework
	HST2 (Figures 4f–4h)	Marly Ls and Ls	- Molluscan wacke- to packstone - Foraminiferal wake- to mudstone at Gr	Bivalve shells, *N.* sp., and at Gr foraminifera such as *Idalina* sp., *Rhabdorites* sp.	Low angle lamination, coral fragments are leached and filled with sparry calcite	Inner lagoon
	SB (Figure 6g)	Ds and Ls	- Dolomudstone at all except Gr - Ferr. burrowed mudstone at Gr	Relics of miliolids, gastropods	Hardground, sharp contact, gradational contact at Gr, dedolomitization	Tidal flat

Table 3. (Continued).

Sequence 3	TST3	Ls, argillaceous Ls	- Bioclastic wacke- to packstone - Bioclastic coralline rudstones at Gr	Echinoid fragments, foraminifera, algae, bryozoans	Cross-bedded, cavernous, lens-shaped corals; cementation and glauconitization	Inner lagoon, back reef
	MFZ	Ls, marly Ls	- Bioclastic bryozoan wackestone in Mk and Qt - Bioclastic coralline boundstone	Bryozoans, *Nummulites* spp., alveolinids, serpulids, echinoids	Massive and fragmented branching corals, cementation, micritization	Outer lagoon and reef framework
	HST3 (Figures 4a, 4b, 5b, 5c)	Sandy shales, sandy siltstones, Ls	- Bioclastic foram. wackestone at Mk, Qt, and Ob - Bioclastic coralline bafflestone, bioclastic foram. grainstone at Gr	*Nummulites* spp., bivalve shells dominated by oysters; whale bones and shark teeth at Wh	Overturned and broken branched and meandroid corals, dissolution, vuggy porosity	Inner lagoon
	SB (Figure 6h)	Ss at Wh, sandy marlstone at Mk, Qt, marly Ls at Ob, Gr	- Poorly fossiliferous mudstone at Ob, Gr	Root casts and brackish marine invertebrates at Wh; scattered quartz grains and iron oxides at Mk, Qt; relics of miliolids, gastropods at Ob, Gr	Gradational contact at Wh; sharp at Mk; hardgrounds at Qt, Ob, and Gr; ferrugination	Tidal flat

S: Sequence, Seq. str.: sequence stratigraphy, TST: transgressive system tract, MFZ: maximum flooding zone, Cs: claystone, HST: highstand system tract, SB: sequence boundary, Ls: limestone, Dl: doloston, Ss: sandstone, Gr: Gebel el Ramliya, Ob: Observatory, Qt: Qattamiya, Mo: Mokattam, Mr: Minqar el Rayan, Wh: Wadi el Hitan, *N.*: *Nummulites*, foram: foraminifera, NWB: normal wave base, FWWB: fair-weather wave base, Qz: quartz.

as *N. bullatus* and *N. discorbinus*. In the Minqar el Rayan section in the Fayum area, this boundary is delineated by changing from *Nummulites* limestone beds to claystone and siltstone beds. This sequence boundary is a type 2 of SB because there is no obvious evidence of subaerial exposure. SB2 lies between tidal flat and inner lagoon deposits on the top of Sequence 1 and is overlain by outer lagoon and shoal deposits at the base of Sequence 2. At the Gebel el Ramliya section SB2 is identified by a conglomeratic bed consisting of dolomite pebbles. At the Observatory section, this boundary is characterized by dolomitized lime mudstone, and in the other studied sections SB2 is marked by a gypsiferous claystone bed at the top of Sequence 1. Correlating this boundary to neighboring countries, we notice that the Bartonian stage is nearly missing in most neighboring countries, such as Libya in the west and Jordan and Saudi Arabia in the east (Farouk et al., 2013) but it has been recorded in Tunisia (Grira, 2014) and other countries in Europe, relating to the influence of glacioeustasy and tectonics (Huyghe et al., 2012). Thus, this SB belongs to type 1 of SBs. The third SB (SB3) at the top of Sequence 2 is in the Eastern Desert and Cairo sections. The boundary is represented by tidal flat deposits of ferruginous and dolomudstone beds. In the Fayum area, SB3 is located between lagoonal carbonate beds and its overlying clastic rocks at the Gehannam Formation. This sequence boundary is similar to SB1 and is considered a type 2 SB. The last sequence boundary, SB4, is recorded at the top of all the studied sections, which is represented by the variation in the lithological characters from marly and sandy limestone rocks belonging to the Middle Eocene to clastic rocks with *Carolia placunoides* shells from the Upper Eocene. In the Fayum area the boundary occurs between the claystone bed of the Gehannam Formation and the nonfossiliferous, gypsiferous, and calcareous sandstone bed of the Birket Qarun Formation. SB4 is widely and well correlatable all over the world (Agnini et al., 2011) and is recorded in some neighboring countries like Jordan (Barbieri et al., 2003; Farouk et al., 2015) and also in most countries of the northern Mediterranean Sea (Bassi et al., 2000), showing clear evidence of subaerial exposure. Therefore, SB4 belongs to type 1 of SBs.

4.2.2. System tracts and depositional sequences

The sequences distinguished in the studied sections are composed of two system tracts including a transgressive system tract (TST) in the lower part and a highstand system tract (HST) in the upper part, bound by a zone of maximum flooding (MFZ). The TST is a retrogradational LFA distinguished where the relative sea level rises and the HST is an aggradational and progradational LFA distinguished where the relative sea level is falling. In our study, vertical changes in the studied parameters, LFAs, and SBs enable us to divide the studied sections into three third-order sequences in the following manner:

Depositional sequence 1 (Figure 3): S1 describes the upper Lutetian stage beds as shown in Figure 2. The sequence is bounded by SB1 and SB2 and starts with transgressive deposits. The main identified fossils in this sequence are *Nummulites bullatus*, *Operculina schwageri*, *Fabiana cassis*, and *Schizaster fourtaui*. In the Gebel el Ramliya section, TST1 consists of an open marine shoal of *Nummulites* grainstone beds with bivalve fragments at the base followed by outer lagoon and back reef bioclastic coralline floatstone, forwards into reef core bioclastic coralline rudstone with echinoid spines and foraminifer tests elucidating the MFZ (Figures 6b and 6c). In the other sections, TST1 begins with shoal open marine bioclastic *Nummulites* beds (Figure 4e) and fossiliferous mudstones alternating with open and deep marine echinoid wackestones (Figures 5d and 5e) and bivalve wacke- to packstone and floatstone beds representing the MFZ. HST1 of S1 is characterized in the Gebel el Ramliya (Figure 5a) by aggregate grains, lithoclasts, peloids, and foraminiferal grain- to rudstones. In the other sections, HST1 is marked by inner lagoon (Figure 4d) bioclastic wacke- to floatstones with oyster shells, gastropods, algae, miliolids, echinoid fragments, and clastic rocks in the Minqar el Rayan section. The sequence is overlain by tidal flat mudstones and gypsiferous claystones (Figure 4c).

Depositional sequence 2 (Figure 3): S2 represents the lower Bartonian stage beds as shown in Figure 2. The index fossils in this sequence are *Tremogastrina fourtaui*, *Dictyoconus egyptiensis*, *Somalina stefaninii*, *Rhabdorites minima*, *Orbitolites* sp., and *Gypsina carteri*. TST2 of S2 in the Gebel el Ramliya and Observatory sections (Figure 3) is marked by back reef bioclastic coralline floatstone (Figures 5h and 6a) and rudstone beds with branching corals, foraminifers, and algae grading into foraminiferal coralline boundstones with huge amounts of coral debris exhibiting the MFZ (Figures 6d and 6e). In the other sections (Figure 3), TST2 consists of shoal molluscan and nummulite beds with other foraminiferal tests and echinoid spines, which are overlain by outer lagoon nummulite bryozoan wacke- to floatstones with bivalves and echinoid fragments. The bryozoan beds mark the MFZ (Figures 5f and 5g). HST2 of S2 in the Gebel el Ramliya section is marked by a progradation from reef to back reef LFA of foraminiferal wackestones with coral fragments and relics of foraminifers. In the other sections, HST2 consists of inner lagoon bivalve and foraminiferal wackestones (Figures 4f–4h) and mudstones that were settled on the outer lagoon beds. HST2 in all the sections is overlain by a tidal flat mudstone bed that represents SB3 (Figures 6f and 6g).

Depositional sequence 3 (Figure 3): S3 makes up the upper part of the upper Bartonian stage beds as shown in Figure 2. The main guide fossils of S3 are *Nummulites*

beaumonti; bivalve shells such as *Ostrea reili*, *Vulsella crispata*, *Lucina pharaons*, *Lucina egyptiaca*, and *Vulsella crispate*; and whale bones such as *Basilosaurus* sp. At the Gebel el Ramliya and the observatory sections, TST3 of S3 start with outer lagoonal bioclastic wackestones with bryozoans (only in Gebel el Ramliya), echinoids, and foraminifers. These are overlain by bioclastic coralline boundstones with branching corals and relics of foraminifera representing the MFZ. At the Qattamiya and Mokattam sections, TST3 is recognized by inner lagoon bioclastic nummulite wackestones with bivalve shells and benthic foraminifers. The HST is overlain by the MFZ of outer lagoon bryozoan beds in the Qattamiya section and shoal nummulite grainstone beds in the Mokattam section. HST3 of S3 in the Gebel el Ramliya and the Observatory sections consists of outer lagoon to shoal bioclastic wackestones and grainstones (Figures 5b and 5c) with alveolinids, corals, and gastropods. In the Qattamiya and Mokattam sections, HST3 is represented by shallowing upward and regressive LFAs of inner lagoon bioclastic wackestones and mudstones with relics of nummulite and oyster shells. S3 in the Wadi el Hitan section is only represented by HST3 and consists mainly of tidal flat clastic rocks (Figures 4a and 4b) with shark teeth and whale bones. The HST3 deposits are overlain by shallow marine inner lagoon deposits in the Gebel el Ramliya and Observatory sections. In the Qattamiya and Mokattam sections the inner lagoon beds are overlain by tidal flat deposits, which represent SB4 (Figure 6h).

4.2.3. Relationship between the studied sequence stratigraphy and diagenesis

The marine deposits of the studied carbonate platform formed in the Middle Eocene over much of northern Egypt include a thick development of corals, bryozoans, bivalve shells, gastropods, and foraminifers and represent cycles of tidal flat, lagoon, shoal, and reef framework carbonates. At the beginning of the Middle Eocene deposition, a marine transgression was prevalent over a large area with a lagoon environment and then was followed by shoal and reef frameworks, which were followed by open marine conditions, where carbonates crowded with various fossils were deposited. The classical sequence stratigraphic model cannot give candid data about the postdepositional development of carbonate rocks. The combination of sequence stratigraphy and diagenesis, however, lets us expect the locative distribution and the age of diagenetic features, and thus gives an understanding of the postdepositional evolution. The diagenesis during transgressive and regressive sequences is strongly influenced by the sedimentological and climatic setting as well as by accommodation changes (Moore 2007). Based on the field observation and detailed analysis, two main factors could control the diagenetic alteration:

1) The primary composition of the components: This factor is considered to have the main effect on the diagenetic alteration and porosity degree of the studied sediments. According to Benito et al. (2001), the original mineralogy of the carbonate sediments controls the intensity of the creation of fabric-selective secondary porosity. The diagenetic leaching, compaction, and also dolomitization are discernable with reference to the mineralogical component as the isopachous cement is arranged in fibrous to bladed crusts and the intensity of cementation may vary strongly, depending on the inner composition of components (aragonite, calcite, high or low magnesium calcite, and the mud content). The preservation could be considered as a result of primary pore-space occlusion that prevents the flow of diagenetic fluids (Flügel, 2010; Palermo et al., 2012). This type of cementation was developing before the dissolving of skeletal components. Other cementation features such as dog teeth and drusy cements have been influenced by meteoric or marine diagenesis. According to Reinhold (1999), the petrographic and geochemical study of the dog tooth cement is not restricted to one specific diagenetic environment. Braun (2003) stated that cements exhibit similar colors with the absence of clear sharp boundaries in addition to gradational transitions between cementation phases, possibly referring to the marine origin of the dog tooth cement. The dissolution of aragonitic bioclasts may lead to the formation of moldic and vuggy porosities and hence the improvement of reservoir quality.

2) Depositional system tracts (long-term average sea level): The study of thin-sections extracted from system tracts revealed that diagenetic alterations are controlled by the TST and HST. By way of example, in the TST, the isopachous cements are usually recorded in the high energy shoal and reef LFAs while the mud content is declining in the transgressive parts. Glauconitization is also related to the TST and the MFZ. The variations in sea level can aid in identifying the clay minerals. The relative sea-level changes help in the type determination and the distribution extent of clay minerals. Thus, during the sea transgression, autochthonous glauconite forms along the MFZ (Worden and Morad, 2003). A rise in relative sea level is accompanied by a decrease in sedimentation rate as in the shoal and the reef LFAs because most of the coarse-grained sediments are dominantly fine-grained and show a progressive upward increase in the amounts of autochthonous glauconite. Brugger et al. (2003) stated that the continuous rise in relative sea level during the deposition of the TST causes a reduction in the subaerially exposed portion of parasequence boundaries, a decrease in the hydraulic head, and a landward migration of the marine pore-water zone, which explains the existence of autochthonous glauconites within the transgressive phase.

Table 4. The relationship between diagenetic features and a sequence stratigraphy of the Middle Eocene in northern Egypt.

Diagenetic process	During transgressive system tract	During highstand system tract
Bioerosion	Micritic envelopes and completely micritized grains are dominant in S2 and S3 (Gebel el Ramliya and Observatory).	Completely and partly micritized grains are recorded in S3 (Qattamiya section)
Dissolution and leaching	In all sequences of Gebel el Ramliya and Qattamiya, but less so than the regressive parts	Dominant in S3 of all sections and also in S1 and S2 (increasing upward)
Cementation	Isopachous and blocky calcite cements usually occur in all S2 and S3 sections (especially in Gebel el Ramliya)	Drusy and blocky calcite crystals are common
Dolomitization	Observed at the base of the deepening upward sequences in all sections	At the shallowing upward sequences in all sections
Dedolomitization	Not recorded	At the end of the shallowing upward sequences in all sections
Neomorphism	Aggrading neomorphism of many skeletal particles is observed in S1 and S3 in the Gebel el Ramliya, Qattamiya, and Minqar el Rayan sections	Aggrading neomorphism of both matrix and skeletal particles is common in all sequences (in some cases associated with sequence boundaries)
Compaction	Mechanical compaction is recorded in all sequences, especially in the Qattamiya section; in a few cases chemical compaction is also recorded in the transgressive part	Chemical compaction is mostly in the Qattamiya and the Mokattam sections; some fractures (mechanical compaction) in *Nummulites* tests are also recorded in S3 in the Qattamiya section
Glauconitization	Mainly recorded here as autochthonous glauconite in the Minqar el Rayan section	Recorded as allochthonous glauconite as in the Qattamiya and Wadi el Hitan sections
Ferrugination	In a few cases, the foraminiferal grains show black impregnation in S2 and S3 in the Observatory and Qattamiya sections	At all sequences at the top of shallowing upward sequences and associated with sequence boundaries
Silicification	Not recorded	At the Fayum sections

At the HST, the dissolutions, chemical compactions, and dolomitization features are all recorded. The dissolution process within the moderate to low energy facies types may be caused by meteoric influence under shallow-water conditions or by $CaCO_3$-undersaturated pore waters (Palermo, 2007). The porosities that have been investigated most in terms of them being interparticle and intraparticle are situated in the middle section between the TST and HST. It is located above the point where the mud content starts to decay while cementation is continuously increasing upward. The HST is accompanied by an increase in sedimentation rate and amounts of mud contents as in the tidal flat and the lagoonal LFAs. The recorded dolomitization within the studied sections could be attributed to the regressive sea level in the mixed phreatic and meteoric zones accompanied with vuggy and moldic porosities (Humphrey, 1988). The mixed marine/meteoric pore water zone is markedly shifted landwards during the relative sea-level fall, which may account for the upward dolomitization increase in regressive carbonate successions (Taghavi et al., 2006). Further evidence for the mixing zone of the dolomitization comes from the lack of associated evaporates, supersaturated with respect to Mg^{2+} (Machel, 2004).

At SBs, the dedolomitization, allochthonous glauconitization, silicification, and ferrugination are all recorded. According to Morad et al. (2000), unconformities that occurred due to the major fall in the relative sea level coincide with basinwards migration of the meteoric pore water zone, which is linked to the diagenesis in carbonate sediments. Dolan (1989) deduced that the increase in sea level decrease is accompanied by an increase in erosion and periods of subaerial exposure. In the studied sections, the transformation of pore water chemistry from

marine to meteoric composition could be attributed to the reverse conversion of dolomite to calcite, i.e. chemical instability of dolomite (e.g., Fretwell et al., 2005). A similar interpretation for the dedolomitization process was suggested by Rameil (2008). He concluded that this type of dedolomitization occurs after long-term emersion events (e.g., large-scale/"3rd-order" SBs). The development and the growth of crystals at higher rates than other crystals during the dedolomitization process might be attributed to a long period of subaerial erosion under the effect of the meteoric environment at the top parts of the HST. The fall in the relative sea level below shelf break may also result in the erosion of autochthonous glauconite and produce allochthonous glauconite (Ketzer et al., 2003). Silicification is recorded in the mixing zone, and the sea regression allows silica ions to be transported farther in a seaward direction, where they could be subject to subsequent filtration through the limestone dolomitization process. This scenario, which could cause a decrease in the pH level and an increase in salinity as well as the CO_2 concentration, may result in the precipitation of silica (Hesse, 1989) and the silica could probably be derived from another terrestrial possible source such as the Upper Eocene sandstone beds during the regressive parts.

5. Conclusions

This study is constructed based on six Middle Eocene stratigraphic sections in northern Egypt. The studied sections are dominated by various facies types and facies associations. These facies associations are vertically arranged in three third-order sequences bounded by four SBs of the lower Lutetian/upper Lutetian boundary, Lutetian/Bartonian boundary, lower Bartonian/upper Bartonian boundary, and Bartonian/Priabonian boundary. Two main factors have been identified as responsible for the diagenetic alterations in the studied sections. The first factor affecting the diagenetic alterations is the primary composition of the components such as mud contents, aragonite, or calcite as the outcome of the primary pore-space blockage as well as the meteoric effectiveness. The second factor is the depositional system tracts. For instance, isopachous cements and autochthonous glauconite are mostly recorded in transgressive system tracts as a result of decreases in both the mud content and the sedimentation rate in the studied sections. In contrast, most of the dissolution, chemical compaction, and dolomitization are recorded in the highstand system tracts as a result of development in mud quantities and sedimentation rate. Dedolomitization, allochthonous glauconitization, silicification, and ferrugination processes have been recorded at SBs as a result of the long-term subaerial erosions.

Acknowledgments

The authors would like to extend their sincere appreciation to the Deanship of Scientific Research at King Saud University for its funding this research group No. (RG-1435-033). The authors are indebted to Thomas Aigner (Tübingen University) for his guidance, support, and advice during this work. We would also especially like to thank Abdelmohsen Ziko (Zagazig University) and Mohram Elgamal (petroleum advisor) for their help in the fieldwork and discussions. Many thanks to Lars Reuning (RWTH-Aachen University) for his final review and the valuable discussions, as well.

References

Abdel-Fattah Z, Gingras M, Caldwell M, Permberton S (2010). Sedimentary environments and depositional characteristics of the Middle to Upper Eocene whale-bearing succession in the Fayum Depression, Egypt. Sedimentology 57: 446-476.

Abu Elghar MS (2012). Sequence stratigraphy and cyclicity in the Middle Eocene of the Fayoum ranges, Western Desert, Egypt: implications for regional sea level changes. Mar Petrol Geol 29: 276-292.

Abu Elghar MS, Hussein AW (2005). Post-depositional changes of the Lower- Middle Eocene limestones of the area between Asuit and Minia, west of the Nile Valley, Egypt. In: First International Conference on the Geology of the Tethys, Cairo University, pp. 123-162.

Adabi M, Zohdi A, Ghabeishavi A, Amiri-Bakhtiyar H (2008). Applications of nummulitids and other larger benthic foraminifera in depositional environment and sequence stratigraphy: an example from the Eocene deposits in Zagros Basin, SW Iran. Facies 54: 499-512.

Agnini C, Fornaciari E, Giusberti L, Grandesso P, Lanci L, Luciani V, Muttoni G, Pälike H, Rio D, Spofforth D et al.(2011). Integrated biomagnetostratigraphy of the Alano section (NE Italy): a proposal for defining the middle-late Eocene boundary. Geol Soc Am Bull 123: 841-872.

Allam A, Shama K, Zalat A (1991). Biostratigraphy of the Middle Eocene succession at Mishgigah, Wadi Rayan, Libyan Desert, Egypt. J Afr Earth Sci 12: 449-459.

Barbieri R, Benjamini C, Monechi S, Reale V (2003). Stratigraphy and benthic foraminiferal events across the middle–late Eocene transition in the western Negev. In: Prothero DR, Ivany LC, Nesbitt, EA, editors. From Greenhouse to Icehouse: The Marine Eocene–Oligocene Transition. New York, NY, USA: Columbia University Press, pp. 453-470.

Basilone L (2009). Sequence stratigraphy of a Mesozoic carbonate platform-to-basin system in western Sicily. Cent Eur J Geo 1: 251-273.

Bassi D, Cosovic C, Papazzoni CA, Ungaro S (2000). The Colli Berici. In: Bassi D, editor. Field Trip Guidebook. Shallow Water Benthic Communities at the Middle–Upper Eocene Boundary. Southern and North-Eastern Italy, Slovenia, Croatia, Hungary. 5th Meeting of the International Geoscience Programme. Ferrara, Italy: IGCP, pp. 43-57.

Bathurst RG (1975). Carbonate Sediments and Their Diagenesis. 2nd ed. Developments in Sedimentology 12. New York, NY, USA: Elsevier.

Benito MI, Lohmann, KC, Mas, R. (2001). Discrimination of multiple episodes of meteoric diagenesis in a Kimmeridgian Reefal Complex, North Iberian Range, Spain. J Sediment Res 71: 380-393.

Boukhary M, Guernet C, Strougo A, Bassoon M, Bignot G, Abdel Ghany O (1993). Eocene ostracods of Mingar El-Rayan (Fayum District, Egypt), stratigraphic and paleogeographic implication. Rev Micropaleont 36: 191-211.

Braithwaite CJ, Montaggioni LF (2009). The Great Barrier Reef: a 700 000 year diagenetic history. Sedimentology: 56: 1591-1622.

Braun S (2003). Quantitative analysis of carbonate sandbodies: outcrop analog study from an epicontinental basin (Triassic Germany). PhD, University of Tübingen, Tübingen, Germany.

Bruggemann J, Buffler R, Guillaume M, Walter R, Cosel R, Ghebretensae B, Berhe S (2004). Stratigraphy, palaeoenvironments and model for the deposition of the Abdur Reef Limestone: context of an important archaeological site from the last interglacial on the Red Sea coast of Eritrea. Palaeogeogr Palaeocl 203: 179-206.

Brugger J, McPhail DC, Wallace M, Waters J (2003). Formation of willemite in hydrothermal environments. Econ Geol 98: 819-835.

Cabioch G, Montaggioni L, Frank N, Seard C, Sall, E, Payri C, Paterne M (2008). Successive reef depositional events along the Marquesas foreslopes (French Polynesia). Mar Geol 254: 18-34.

Catuneanu O, Abreu V, Bhattacharya J, Blum M, Dalrymple R, Eriksson P, Fielding C, Fisher W, Galloway W, Gibling M et al. (2009). Towards the standardization of sequence stratigraphy. Earth-Sci Rev 92: 1-33.

Dolan JF (1989). Eustatic and tectonic controls on deposition of hybrid siliciclastic/carbonate basinal cycles: discussion with examples. AAPG Bull 73: 1233-1246.

Dulo WC (1986). Variation in diagenetic sequences: an example from Pleistocene coral reefs, Red Sea, Saudi Arabia. In: Schroeder JH, Purser BH, editors. Reef Diagenesis. Berlin, Germany: Springer-Verlag, pp. 77-90.

El Ayyat AM (2013). Sedimentology, sequential analysis 409 and clay mineralogy of the lower Eocene sequence at Farafra Oasis area, Western Desert of Egypt. J Afr Earth Sci 78: 28-50.

El-Azabi MH (2006). Sedimentological characteristics, palaeoenvironments and cyclostratigraphy of the middle Eocene sequences in Gabal el-Ramliya, Maadi-Sukhna stretch, north eastern Desert. In: Egyptian 8th International Conference on the Geology of Arab World, Cairo, Egypt, pp. 1-31.

El-Fawal FM, El-Asmar HM, Sarhan MA (2013). Depositional evolution of the Middle-Upper Eocene rocks, Fayum area, Egypt. Arab J Geo 6: 749-760.

Embry AF, Johannessen EP (1992). T–R sequence stratigraphy, facies analysis and reservoir distribution in the uppermost Triassic–Lower Jurassic succession, western Sverdrup Basin, Arctic Canada. In: Vorren TO, Bergsager E., Dahl-Stamnes OA, Holter E, Johansen B, Lie E, Lund TB, editors. Arctic Geology and Petroleum Potential. Norwegian Petroleum Society Special Publication. Amsterdam, the Netherlands: Elsevier, pp. 121-146.

Embry AF, Klovan JE (1971). A Late Devonian reef tract on northeastern Banks Island, Northwest Territories. Bull Can Pet Geol 33: 730-781.

Emery D, Myers KJ (1996). Sequence Stratigraphy. Oxford, UK: Blackwell Science.

Evans CC, Ginsburg RN (1987). Fabric-selective diagenesis in the Late Pleistocene Miami Limestone. J Sediment Petrol 57: 311-318.

Farouk S, Ahmad F, Smadi, AA (2013). Stratigraphy of the Middle Eocene–Lower Oligocene successions in northwestern and eastern Jordan. J Asian Earth 73: 396-408.

Farouk S, Faris M, Ahmad F (2015). New microplanktonic biostratigraphy and depositional sequences across the Middle–Late Eocene and Oligocene boundaries in eastern Jordan. GeoArabia 20: 145-172.

Flügel E (2004). Microfacies of Carbonate Rocks: Analysis, Interpretation and Classification. Berlin, Germany: Springer-Verlag.

Flügel E (2010). Microfacies Analysis of Limestones. Berlin, Germany: Springer Science & Business Media.

Fretwell BA, Burgessa WG, Barker JA, Jefferies NL (2005). Redistribution of contaminants by a fluctuating water table in a micro-porous, double-porosity aquifer: field observations and model simulations. J Contam Hydrol 78: 27-52.

Gingerich PD (1992). Marine Mammals (Cetacea and Sirenia) from the Eocene of Gebel Mokattam and Fayum, Egypt; Stratigraphy, Age and Paleoenvironments. Ann Arbor, MI, USA: University of Michigan Papers of Paleontology.

Gradstein FM, Ogg JG, Schmitz M, Ogg G (2012). The Geologic Time Scale 2012. Amsterdam, the Netherlands: Elsevier.

Grira C (2014). Biostratigraphy of the Lutetian/Bartonian Boundary in the North of Tunisia. Rend Soc Geol Ital 31: 93-94.

Gvirtzman G, Friedman GM (1977). Sequence of progressive diagenesis in coral reefs: submerged modern reefs to emerged Pleistocene reefs. AAPG 4: 357-380.

Haggag MA (1990). *Globigerina pseudoampliapertura* zone, a new late Eocene planktonic Foraminiferal zone (Fayoum area, Egypt). Neues Jahrb Geol: 295-307.

Haggag MA (1992). A comprehensive Egyptian Middle/Upper Eocene planktonic foraminiferal zonation. Egypt J Geol 36: 97-118.

Haq BU, Hardenbol J, Vail PR (1987). Chronology of fluctuating sea levels since the Triassic. Science 235: 1156-1167.

Helal SA (1990). Stratigraphic and paleontologic studies of the Eocene sediments in Gabel Shbraweet area, Eastern Desert, Egypt. MSc, Ain Shams University, Cairo, Egypt.

Helal SA (2002). Contribution to the Eocene benthic foraminifera and Ostracoda of the Fayum Depression, Egypt. Egypt J Paleontol 2: 105-155.

Hesse R (1988). Origin of chert, I. Diagenesis of biogenic siliceous sediments. Geo Can 15: 171-192.

Humphrey JD (1988). Late Pleistocene mixing zone dolomitization, southeastern Barbados, West Indies. Sedimentology 35: 327-348.

Huyghe D, Castelltort S, Mouthereau F, Serra-Kiel J, Filleaudeau PY, Emmanuel L, Berthier B, Renard M (2012). Large scale facies change in the middle Eocene South-Pyrenean foreland basin: the role of tectonics and prelude to Cenozoic ice-ages. Sediment Geol 253: 25-46.

Johannesson KH (2012). Rare earth element geochemistry of scleractinian coral skeleton during meteoric diagenesis: a sequence through neomorphism of aragonite to calcite. Sedimentology 56: 1433-1463.

Ketzer JM, Holz M, Morad S, Al-Aasm IS (2003). Sequence stratigraphic distribution of diagenetic alterations in coal-bearing, paralic sandstones: evidence from the Rio Bonito Formation (early Permian). South Bra Sedi 50: 855-877.

Khalifa MA, El Ghar MA, Al Aasm I (2014). Linking carbonate cyclicity in platforms to depositional and diagenetic overprints: an example from the Lower Eocene Drunka Formation, west of Assiut-Minia stretch, Western Desert, Egypt. Arabian Journal of Geosciences 7: 5159-5170.

Koch R, Zinkernagel N (1996). Zur Zementation in Kalksteinen. Zbl Geol Paläontol 11/12: 1353-1398 (in German).

Kovacs JS (2005). Depth gradient proxies: palaeoecology versus sedimentology. Case study from the Turea Group deposits of the Paleogene Transylvanian Basin. Acta Palaeontol Roman 5: 259-276.

Lotfy H, Van der Voo R (2007). Tropical northeast Africa in the middle-late Eocene: paleomagnetism of the marine mammals sites and basalts in the Fayum province, Egypt. J Afr Earth Sci 47: 135-152.

Machel HG (2004). Concepts and Models of Dolomitisation: A Critical Reappraisal. London, UK: Geological Society of London Special Publications.

Marzouk AM, El Shishtawy AM, Kasem AM (2014). Calcareous nannofossil and planktonic foraminifera biostratigraphy through the Middle to Late Eocene transition of Fayum area, Western Desert, Egypt. J Afr Earth Sci 100: 303-323.

Moore CH (2007). Carbonate Reservoirs, Porosity Evolution and Diagenesis in a Sequence Stratigraphic Framework. Amsterdam, the Netherlands: Elsevier.

Morad S (1998). Carbonate sedimentation in sandstone: distribution patterns and geochemical. In: Morad S, editor. Carbonate Cementation in Sandstone. Gent, Belgium, International Association of Sedimentologists, pp. 1-26.

Morad S, Ketzer JR, De Ros LF (2000). Spatial and temporal distribution of diagenetic alterations in siliciclastic rocks: implications for mass transfer in sedimentary basins. Sedimentology 47: 95-120.

Morad S, Ketzer JR, De Ros LF (2012). Linking Diagenesis to Sequence Stratigraphy (Special Publication 45 of the IAS). New York, NY, USA: John Wiley & Sons.

Mostafa A, Hassan AM (2004). Sequence stratigraphy and depositional history of some Mesozoic-Cenozoic succession in the Gulf of Suez and north Western Desert, Egypt. In: Proceedings of the 14th Symposium on Phanerozoic and Development in Egypt, pp. 27-58.

Nichols G (1999). Sedimentology and Stratigraphy. Oxford, UK: Blackwell.

Nothdurft L (2007). Microstructure and early diagenesis of recent reef building scleractinian corals, Heron reef, Great Barrier Reef: implication for palaeoclimate analysis. PhD, Queensland University of Technology, Brisbane, Australia.

Nothdurft L, Webb GE (2009). Earliest diagenesis in scleractinian coral skeletons: implications for palaeoclimate-sensitive geochemical archives. Facies 55: 161-201.

Omar AA (1999) Benthic foraminifers of Wadi El Rayan, area, Fayum Province, Egypt (Stratigraphy and Paleoecology). In: GAW4 International Conference of the Arab World, Cairo, Egypt, pp. 905-923.

Palermo D (2007). Anatomy of Carbonate Sandbodies: Reservoir Analog Study from an Epicontinental Basin (Triassic, Germany). Tübingen, Germany: Tübingen University.

Palermo D, Aigner T, Seyfang B, Nardon S (2012). Reservoir properties and petrophysical modelling of carbonate sand bodies: outcrop analogue study in an epicontinental basin (Triassic, Germany). Geol Soc Spec Publ 370: 111-138.

Rameil N (2008). Early diagenetic dolomitization and dedolomitization of Late Jurassic and earliest Cretaceous platform carbonates: a case study from the Jura Mountains (NW Switzerland, E France). Sed Geol 212: 70-85.

Reinhold C (1999). Dog-tooth cements; indicators of different diagnetic environments. Zbl Geol Paläont 10-12: 1221-1235.

Said R (1990). The Geology of Egypt**.** Rotterdam, the Netherlands: Balkema.

Sallam E, Issawi B, Osman R (2015a). Stratigraphy, facies, and depositional environments of the Paleogene sediments in Cairo-Suez district, Egypt. Arabian Journal of Geosciences 8: 1939-1964.

Sallam E, Wanas HA, Osman R (2015b). Stratigraphy, facies analysis and sequence stratigraphy of the Eocene succession in the Shabrawet area (north Eastern Desert, Egypt): an example for a tectonically influenced inner ramp carbonate platform. Arabian Journal of Geosciences 8: 10433-10458.

Schandelmeier H, Reynolds P, Semtner, AK (1997). Palaeogeographic-Palaeotectonic Atlas of North-Eastern Africa, Arabia and Adjacent Areas. Rotterdam, the Netherlands: Balkema.

Sedgwick PE, Davis RA (2003). Stratigraphy of washover deposits in Florida: implications for recognition in the stratigraphic record. Mar Geol 200: 31-48.

Shen JW, Webb GE, Jell JS (2008). Platform margins, reef facies, and microbial carbonates; a comparison of Devonian reef complexes in the Canning Basin, Western Australia, and the Guilin region, South China. Earth-Sci Rev 88: 33-59.

Steinhauff DM, Walker KR, Goldberg SA (1999). Diagenesis by burial fluids, Middle Ordovician Platform to Platform-Margin limestones, East Tennessee: relationship to Mississippi Valley-type deposits. J Sediment Res 69: 1107-1122.

Strasser A, Stromhmenger C (1997). Early diagenesis in Pleistocene coral reefs, southern Sinai, Egypt; response to tectonics, sea-level and climate. Sedimentology 44: 537-558.

Strougo A (1985a). Eocene Stratigraphy of the eastern Greater Cairo (Gebel Mokattam-Helwan) area. Middle East Research Center Ain Shams University Earth Science Series 5: 1-39.

Strougo A (1985b). Eocene stratigraphy of the Giza Pyramids plateau. Middle East Research Center Ain Shams University Earth Science Series 5: 79-99.

Strougo A (2008). The Mokattamian Stage. Middle East Research Center Ain Shams University Earth Science Series 22: 47-108.

Strougo A, Abd-Allah AM (1990). Mokattamian stratigraphy of north central Eastern Desert (south of Maadi-Qattamiya road). Middle East Research Center Ain Shams University Earth science Series 4: 152-175.

Strougo A, Azab MM (1991). Bivalve molluscs from a lower Mokattamian (Middle Eocene) shell bed at the base of the Midawara Formation of Gebel el Mehasham, Magahaga area. Middle East Research Center Ain Shams University Earth Science Series 5: 95-119.

Strougo A, Bignot G, Abd-Allah AM (1992). Biostratigraphy and paleoenvironments of Middle Eocene benthic foraminiferal assemblages of the north central Eastern Desert, Egypt. Middle East Research Center Ain Shams University Earth Science Series 6: 1-12.

Strougo A, Boukhary MA (1987). The middle Eocene-upper Eocene boundary in Egypt: present state of problem. Revue de Micropaleontologie 30: 122-127.

Taghavi AA, Mork A, Emadi MA (2006). Sequence stratigraphically controlled diagenesis governs reservoir quality in the carbonate Dehluran Field, southwest Iran. Petroleum Geoscience 12: 115-126.

Tawfik M, El-Sorogy AS, Moussa M (2016). Metre-scale cyclicity in Middle Eocene platform carbonates in northern Egypt: Implications for facies development and sequence stratigraphy. J Afr Earth Sci 119: 238-255.

Tucker ME, Booler J (2002). Distribution and geometry of facies and early diagenesis: the key to accommodation space variations and sequence stratigraphy: upper cretaceous congest carbonate platform, Spanish Pyrenees. Sed Geol 146: 225-247.

Uhen MD (2004). Form, Function, and Anatomy of *Dorudon atrox* (Mammalia, Cetacea): An Archaeocete from the Middle to Late Eocene of Egypt. Ann Arbor, MI, USA: University of Michigan Papers of Paleontology.

Vail PR, Mitchum RM Jr, Thompson S (1977). Seismic stratigraphy and global changes of sea level, part 4: global cycles of relative changes of sea level. Am Assoc Petr Geol 26: 83-97.

Van Woesik R, van Woesik K, van Woesik L, van Woesik S (2013). Effects of ocean acidification on the dissolution rates of reef-coral skeletons. PeerJ 1: 208.

Wallace MW, Kerans C, Playford PE, Mcmanus A (1991). Burial diagenesis in the Upper Devonian reef complexes of the Geikie Gorge region, Canning Basin, Western Australia. AAPG Bull 75: 1018-1038.

Worden RH, Morad S (2003). Clay Minerals in Sandstones: Controls on Formation, Distribution and Evolution. Oxford, UK: Blackwell Publishing, Ltd.

Ziko A (1985). Eocene Bryozoa from Egypt. PhD, Tübingen University, Tübingen, Germany.

Zonneveld JP, Gingras MK, Pemberton SG (2001). Trace fossil assemblages in a Middle Triassic mixed siliciclastic-carbonate marginal marine depositional system. British Columbia. Palaeogeogr Palaeoclimatol Palaeoecol 166: 249-276.